

Al-Quds University
Deanship of Graduate Studies
Physics Department



**Gamma-Ray Measurements of Soil Samples from
Southern Parts of Bethlehem up to Southern Parts of
Hebron in Palestine**

Ahmad Hilmi Abdel Hadi Shatat

M. Sc. Thesis

Jerusalem-Palestine

1437/2016

**Gamma-Ray Measurements of Soil Samples from
Southern Parts of Bethlehem up to Southern Parts of
Hebron in Palestine**

Name: Ahmad Shatat
B.Sc. Physics, Beirziet University, Palestine

Supervisor:

Dr. Othman H Y Zalloum
Associate Professor of Physics
Palestine Polytechnic University, Hebron, Palestine

Thesis Submitted in Partial Fulfillment of Requirements for
the Degree of Master of Science in Physics

Al-Quds University

1437/2016

Al– Quds University
Deanship of Graduate Studies
Physics Department



Thesis Approval

Gamma-Ray Measurements of Soil Samples from Southern Parts of Bethlehem up to Southern Parts of Hebron in Palestine

Prepared by: Ahmad Hilmi AbdelHadi Shatat

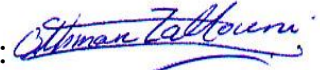
Registration No: 20812431

Supervisor:

Dr. Othman H Y Zalloum
Associate Professor of Physics
Palestine Polytechnic University, Hebron, Palestine

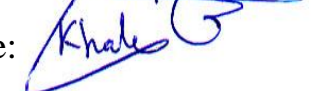
Master thesis submitted and accepted, 11 /07 /2016, Names and signatures of
examining committee members:

1. Head of the committee: Dr. Othman H. Y. Zalloum
2. Internal Examiner: Dr. Hussein Al-Samamrah
3. External Examiner: Dr. Dr. Khalil Thabaineh

Signature: 

Signature:

Signature: 

Signature: 

Jerusalem-Palestine

1437/2016

بِسْمِ اللّٰهِ الرَّحْمٰنِ الرَّحِیْمِ

وَقَالَ فِرْعَوْنُ اِنْتُونِي بِكُلِّ سَاحِرٍ عَلِيمٍ (79) فَلَمَّا جَاءَ السَّحَرَةُ قَالَ لَهُمْ مُوسَى اَلْقُوا مَا اَنْتُمْ مُنْقُونَ (80) فَلَمَّا اَلَقُوا قَالَ مُوسَى مَا جِئْتُمْ بِهٖ سِحْرٍ ۗ اِنَّ اللّٰهَ سَيُبْطِلُهُ ۗ اِنَّ اللّٰهَ لَا يُصْلِحُ عَمَلَ الْمُفْسِدِيْنَ (81) وَيُحِقُّ اللّٰهُ الْحَقَّ بِكَلِمَاتِهٖ وَلَوْ كَرِهَ الْمُجْرِمُونَ.

سورة يونس

Dedication

To those who dig hard for the truth, balance and justice. To those who build up their righteous principles and stand firm for that against internal and external storms of dirt. Upon all those is my master Mohammad" peace be upon him and could be attained but through him" who did his best to build up humanity clean principles.

Declaration

I certify that the work presented in this thesis for the degree of master science in physics in the result of my efforts, and not have been presented for a higher degree to any other university or institution.

Signed : 

Ahmad Hilmi Abdel Hadi Shatat

Date:

Acknowledgments

Praise is due to Allah for helping me.

Great thanks should be due to Dr. Sari Nusaibah, to his office manager Mr. Mohammad Hussain and to Dr. Sa'eed Zeedani who all represent the ideal team to put this institution on the track of freedom, independence, productivity and progress. I was all the time since 2008 being blocked from achievement, and on the other hand I was in all that time being covered by such a team that Dr. Sari was on top of.

I wish to express my sincere gratitude to my supervisor, Dr. Othman H. Y. Zalloum who assisted my work with many helpful comments and discussions, but nevertheless left me the freedom to pursue my own ideas as well.

My thanks are also due to Mr. Ismael Hroub the Manager at Palestinian Ministry of Health and the head of the Radiation Protection and Detection Unit - Palestinian Ministry of Health and the National Liaison Officer (NLO) to Palestine at International Atomic Energy Agency (IAEA) and to his assistant Mr. Ra'fat Odeh in the Radiation Protection and Detection Unit in the Palestinian Ministry of Health for their help and cooperation in the Gamma spectroscopy laboratory using the NaI(Tl) system, where it is true that I was dependent on their experience in running the system and acquiring the spectra.

My thanks and appreciation also goes to Dr. Hanna Hallaq of Bethlehem University, who paid much effort to supervise my previous project on X-ray absorption fine structure (XAFS) beamline.

My thanks also goes to Dr. Salman Salman who arranged for my visit to SESAME in which I came back from there with nothing but experience.

Finally, my thanks extends to Dr. Mohammad Abu Samra and to Dr. Khalil Thabayneh for their published work that was beneficial to the project and to Dr. Husain Alsamamra; the Chair of the Physics Department at Al-Quds University, and last but not least to Dr. Elias Elias as a representative to honesty and morals.

Abstract

The aim of this study is to measure the radioactive level relative to destination, where we managed to collect 4 samples from South Bethlehem, 4 samples from north Hebron, and 10 samples from south Hebron and in each of these three main destinations samples were collected from east to west. These samples were measured with the sodium iodide doped with thalium detector (NaI(Tl)).

After making the proper calculations for the main chain serieses of ^{238}U , ^{235}U and ^{232}Th , and ^{40}K natural isotope, and artificial ^{137}Cs radioisotope, we obtained the following values averaged over samples ((57.0±9.7), (3.151±0.326), (47.9±6.0), (78±8.9), and (1.2±0.1)) BqKg^{-1} respectively, where these values showed to be close enough to worldwide averages and ranges.

In addition to that radioactive gauge values which demonstrates the levels of safety were calculated, and these values in successive are: Radium equivalent activity with a value of (131.5±15.1) BqKg^{-1} , Absorbed dose rate in air with a value of (59.4±6.7) nGy/h , Absorbed dose rate in air considering ^{137}Cs and cosmic radiation effects with a value of (93.4±6.7) (nGy/h), Annual effective dose equivalent with a value of (0.481±0.0114) (mSvy^{-1}), External hazard index with a value of (0.3551±0.0407), Internal hazard index with a value of (0.5092±0.0663), and Radioactivity level index with a value of (0.9108±0.0150) where the last three values are relative numbers with no units where all these values are within the averages and ranges of worldwide values.

In addition to that, many of the isotopes of airborne effluents that are usually due to nuclear power plants and the nuclear tests where found, among these effluents where J_{135} , which showed up in most of the samples with an average activity over samples of (66.596±8.524) BqKg^{-1} , and the isotopes (Nb-95, Mo-99, Sb-125, J-131, Cs-134 and Ba-140), with activities successively and respectively (1.242±0.135, 116.001±15.161, 42.351±12.934, 14.01±0.7, 134.756±32.867 and 34.977±8.181) BqKg^{-1} .

List of Contents

سورة يونس 4	
Dedication.....	i
Declaration.....	ii
Acknowledgments.....	iii
Abstract.....	vi
List of Figures.....	x
List of Appendices.....	xii
Definitions.....	xiii
Abbreviations.....	xvi
Chapter One.....	2
Gamma radiation phenomena and its manifestations.....	2
1.1 Introduction.....	2
1.2 Radiation.....	4
1.3 Gamma radiation.....	12
1.3.1 Theory behind gamma ray phenomena.....	12
1.3.2 Gamma radiation interaction with matter.....	14
1.3.2.1 Photoelectric effect.....	15
1.3.2.2 Compton scattering.....	16
1.2.1.1 Pair production.....	17
1.2.1.2 Fluorescent X-ray.....	18
1.4 Radiation Dosimetry.....	19
1.4.1 Activity.....	19
1.4.2 Intensity.....	19
1.4.3 Exposure.....	21
1.4.4 Absorbed dose, dose equivalent, and dose rate.....	22
1.5 Biological Effects of Radiation.....	22
1.6 Gamma ray and medication.....	23
1.7 Study motivations.....	25
1.8 Previous studies in Palestine.....	25

Chapter Two.....	29
Experimental Equipments and Procedures.....	29
2.1 Introduction.....	29
2.2 Samples and the Destinations of collection.....	29
2.3 Experimental setup.....	31
2.3.1 905-3 NaI(Tl) Scintillation Detector.....	32
2.3.2 Multichannel analyzer.....	36
2.3.3 High voltage power supply.....	36
2.4 Calibration.....	37
2.4.1 Energy calibration.....	37
2.4.2 Efficiency calibration.....	39
2.5 Measurement of background.....	44
2.6 Sample measurement and analysis.....	44
Chapter Three.....	47
Theoretical calculations in relation to activity.....	47
3.1 Introductory to activity concentrations calculation.....	47
3.2 Calculation of dose rates and indices.....	48
3.2.1 Radium equivalent activity.....	48
3.2.2 Absorbed dose rate in air.....	48
3.2.3 Annual effective dose equivalent.....	49
3.2.4 External hazard index.....	50
3.2.5 Internal hazard index.....	50
3.2.6 Radioactivity level index.....	50
3.3 Details about contamination products.....	50
Chapter Four.....	54
Results, Reasoning, Comparasions, and Conclusions.....	54

4.1	Introduction.....	54
4.2	Results of NORM.....	54
4.2.1	Results and comparasions of U-238, Th-232, K-40, and Cs-137.....	54
4.2.2	Results of dose parameters and indices.....	56
4.2.3	U-235 activity concentration.....	57
4.3	Results and comparasions of contamination elements.....	57
4.3.1	J-135.....	57
4.3.2	Other fission yeild elements.....	58
	Chapter Five.....	62
	Conclusions and Future work.....	62
5.1	Introduction.....	62
5.2	Future work.....	62
	Appendix A.....	64
	Appendix B.....	64
	Appendix C.....	70
	References.....	71

List of Tables

Table 2.1: (MBSS 2) Reference Nuclides	38
Table 2.2: Resulting energy versus channel number of the used reference nuclides	39
Table 2.3: Resulting efficiencies versus reference energy peaks used	41
Table 2.4: U-238 Daughters peaks with their efficiencies and probabilities of appearance shown	42
Table 2.5: Th-232 Daughters peaks with their efficiencies and probabilities of appearance shown	43
Table 2.6: U-235 Daughter (TH-227) peaks with their efficiencies and probabilities of appearance shown	43
Table 2.7: K-40 isotope peak probability and efficiency	43
Table 2.8: Cs-137 isotope peak probability and efficiency	44
Table 2.9: J-135 peaks with their efficiencies and probabilities of appearance shown	44
Table 2.10: Contamination nuclides with their peaks probabilities and efficiencies shown	44
Table 3.1: Diagnosed peaks of each of U-238, Th-232 and U-235 daughter nuclides	49
Table 3.2: J-135 diagnosed peaks with the sample codes that each peak was found in	52
Table 3.3: Fission product yeild nuclides peaks diagnosed with codes of the samples they were found in	52
Table 4.1: Activity concentration of NORM nuclides and Cs-137 compared to national values	55
Table 4.2: Radiation dose parameters average values compared to worldwide values	57
Table 4.3: Results of U-235 activity concentrations in average form through its duaghter nuclide Th-227	57

List of Figures

Figure 1. 1 The plot of parent and daughter activity in secular equilibrium [1]	9
Figure 1. 2: U-238 decay chain series	10
Figure 1. 3: Th-232 decay chain series	11
Figure 1. 4: U-235 decay chain series	17
Figure 1. 5: Schematic diagram of Compton Effect kinematics [2]	18
Figure 1. 6: Total photon cross section in lead as a function of energy[3]	21
Figure 1.7: Intinsity manipulation across 905-3 NaI(Tl)	29
Figure 2. 1: The three main areas of study circled and named	30
Figure 2. 2: Distinations of collection of samples c1 through c4 circled as shown	30
Figure 2. 3: Distinations of collection of samples b1 through b4 circled as shown	31
Figure 2. 4: Distinations of collection of samples a1 through 10 circled as shown	32
Figure 2. 5: A typical experimental setup for determination of γ -radiation spectrum	32
Figure 2. 6: (a) The fourteen pin connector of the 905-3 NaI(Tl). (b) 905-3 NaI(Tl) [4]	33
Figure 2. 7: Electrical circuit design of the fourteen pinconnector, they connects to the cathode and anodes within the PMT[4]	34
Figure 2. 8: Detecting material Efficiency as a Function of Energy	35
Figure 2. 9: A demonstrative drawing for the mechanisms of 905-3 NaI(Tl) [5]	39
Figure 2. 10: Reference spectrum	40
Figure 2. 11: Resulting energy versus channel number of the used reference nuclides	41
Figure 2. 12: Resulting effeciencies versus reference energy peaks used	44
Figure 2. 13: Resulting background spectrum	45
Figure 2. 14: Resulting spectrum for sample one as a typical form	58
Figure 4. 1: Contamination isotopes found in our samples without including J-135 and Cs-137 versus concentration activity chart	59
Figure 4. 2: Yield of different elements from nuclear fission after different cooling times. This is only a rough estimate. The author did not specify the parent nuclide	59
Figure 4. 3: Contamination isotopes found in our samples including J-135 and Cs-137 versus concentration activity chart	59

List of Appendices

Appendix A64

Table A :The list of sample's site of collection addresses 64

Appendix B65

Table B1: Concentration activities of NORM nuclides and ^{137}Cs 65

Table B2: Results of Radium equivalent activities (Ra_{eq}), outdoor air absorbed, dose (D_r) with ^{137}Cs in consideration and D_r for NORM nuclides only 66

Table B3: Results of annual effective doses out and indoor 67

Table B4: Results of external and internal Hazard indices, and radioactivity level index 68

Table B5: Results of concentration activities for ^{235}U through its daughter nuclide ^{227}Th 69

Appendix C70

Table C1: Results of concentration activities for J_{135} 70

Table C2: Effluents activity concentrations of nuclear events in samples 70

Definitions

- **Absorbed Dose:** Absorbed dose is the amount of energy that ionizing radiation imparts to a given mass of matter. The SI unit for absorbed dose is the gray (Gy), but the “rad” (Radiation Absorbed Dose) is commonly used. 1 rad is equivalent to 0.01 Gy (NDT) [6].
- **Activity:** It is the rate at which the isotope decays. Specifically, it is the number of atoms that decay and emit radiation in one second (NDT) [6].
- **Alpha Particle (α):** An alpha particle is a positively charged particle consisting of two protons and two neutrons emitted from the nuclei of various radionuclides (University) [7].
- **Background radiation:** ionizing radiation from natural sources, such as terrestrial radiation due to radio nuclides in the soil or cosmic radiation originating in outer space (CDC) [8].
- **Becquerel (Bq):** It is that quantity of radioactive material in which one atom transforms per second. It is the (SI) unit for activity (NDT) [6].
- **Beta Particle (β):** Beta particles are negatively charged particles emitted from the nuclei of various radionuclides. A beta particle is identical to an electron.
- **Compton Effect:** The Compton Effect is the quantum theory of the scattering of electromagnetic waves by a charged particle in which a portion of the energy of the electromagnetic wave is given to the charged particle in an elastic, relativistic collision (Parks 2015) [2].
- **Contamination (radioactive):** the deposition of unwanted radioactive material on the surfaces of structures, areas, objects, or people where it may be external or internal (CDC) [8].
- **Decay chain (decay series):** the series of decays that certain radioisotopes go through before reaching a stable form. For example, the decay chain that begins with uranium-238 (U-238) ends in lead-206 (Pb-206), after forming isotopes, such as uranium-234 (U-234), thorium-230 (Th-230), radium-226 (Ra-226), and radon-222 (Rn-222) (CDC) [8].
- **Dose:** Dose describes the amount of energy deposited into a specified mass of material (NDT) [6].

- **Dose Equivalent:** The dose equivalent relates the absorbed dose to the biological effect of that dose. The absorbed dose of specific types of radiation is multiplied by a "quality factor" to arrive at the dose equivalent. The SI unit is the sievert (SV), but the rem is commonly used (NDT) [6].
- **Dose Rate:** Absorbed dose delivered per unit time (CDC) [8].
- **Electric dipole moment:** The electric dipole moment for a pair of opposite charges of magnitude q is defined as the magnitude of the charge times the distance between them and the defined direction is toward the positive charge.
- **Exposure:** The amount of ionization in air produced by the radiation is called the exposure. Exposure is expressed in terms of a scientific unit called a roentgen (R or r) (NDT) [6].
- **Fluorescent X-ray:** (XRF) is the emission of characteristic "secondary" (or fluorescent) X-rays from a material that has been excited by bombarding with high-energy X-rays or gamma rays (Kirz) [3].
- **Gamma Rays (γ):** Gamma rays are electromagnetic radiation emitted from the nuclei of various radionuclides.
- **Gray:** The unit of radiation dose primarily used everywhere else! One Gy is equal to 1 joule of energy deposited into 1 kg of material. 1 Gy is equal to 100 rads (NDT) [6].
- **Half-life:** The half-life ($T_{1/2}$) of a radioactive material is the amount of time it takes for the activity to decrease to $\frac{1}{2}$ of its original amount (CDC) [8].
- **Intensity:** Radiation intensity is the amount of energy passing through a given area that is perpendicular to the direction of radiation travel in a given unit of time (NDT) [6]
- **Ionizing Radiation:** Radiation that has the ability to remove orbital electrons from an atom (ionization) (CDC) [8].
- **Isotope:** Atoms having the same number of protons, but different numbers of neutrons (CDC) [8].
- **Magnetic moment:** Magnetic moment of a magnet is a quantity that determines the torque it will experience in an external magnetic field.
- **Pair production:** Third factor is the pair production. Pair production is the evolution of an electron and a positron out of gamma ray interaction with the nucleus potential or even with that of an electron. The criteria for pair production is

that the gamma ray energy should be equal to the rest mass of the two created particles.

- **Photoelectric effect:** refers to the emission, or ejection, of electrons from the surface of, generally, a metal in response to incident light.
- **Radiation:** The propagation of energy through space, or some other medium, in the form of electromagnetic waves or particles (CDC) [8].
- **Radiation Energy:** Each disintegration results in a release of energy which can be deposited into an absorber.
- **Radiation weighting factor:** The factor by which the absorbed dose (rad or gray) must be multiplied to obtain a quantity that expresses, on a common scale for all ionizing radiation, the biological damage (rem or sievert) to the exposed tissue.
- **Radioactive Decay:** Radioactive decay is the disintegration of an unstable atom with an accompanying emission of radiation.
- **Radioactive Materials:** Radioactive materials are materials that emit ionizing radiation.
- **Radium (Ra):** A radioactive metallic element with atomic number 88. As found in nature, the most common isotope has a mass number of 226. It occurs in minute quantities associated with uranium in pitchblende, carnotite, and other minerals.
- **Risk:** In many health fields, risk means the probability of incurring injury, disease, or death. Risk can be expressed as a value that ranges from zero (no injury or harm will occur) to one (harm or injury will definitely occur).

Abbreviations

- Analogue to Digital Converter (ADC)
- Absorbed dose rate in air (D_r)
- Analogue to Digital Converter (ADC)
- Annual Effective Dose Equivalent (AEDE)
- Boron Neutron Capture Therapy (BNCT)
- Deoxyribonucleic Acid (DNA)
- External hazard index (H_{ex})
- Fast Neutron Therapy (FNT)
- Full Width at Half Maximum (FWHM)
- High Purity Germanium Detector (HPGE)
- Indoor Annual Effective Dose Equivalent (D_{indoor})
- Internal hazard index (H_{in})
- International Atomic Energy Agency (IAEA)
- Minimum Detectable Activity (MDA)
- Multi Channel Analyzer (MCA)
- Naturally Occurring Radioactive Materials (NORM)
- Non Destructive Testing (NDT)
- Nuclear Safeguards industry (NUCSAFE)
- Peak Background Correction (PPC)
- Photo multiplier tube (PMT)
- Radioactivity level index (I_γ)
- Radium Equivalent Activity ($R_{a_{eq}}$)
- Region of Interest (ROI)
- Sodium Iodide doped with Thallium detector (NaI(Tl))
- United Nations Scientific Committee on the Effects of Atomic Radiation (UNSCEAR)

Chapter One

Gamma Radiation phenomena and its manifestations

Chapter One

Gamma radiation phenomena and its manifestations

1.1 Introduction

Radiation as natural phenomena has been under study for a long time. Radiation has two main sources, first is the natural radiation, which could be divided into primordial or terrestrial and cosmogenic (extra terrestrial); second is the man made or artificial radiation, this second source is known to be dangerous because of the high concentration of the radiating materials and because it is being disposed close to earth surface and close to inhabited places.

This branch of study started to appear by the time X-ray was discovered in 1895, a short time after that scientist experienced the fatal results of working with radiation. Many of the pioneers in radiation research became martyrs to their work. In 1928, at the Second International Congress of Radiology, the International Commission on Radiological Protection (ICRP) was set up (Flakus) [9]. ICRP is an independent international organization with more than two hundred volunteer members from approximately thirty countries across six continents(ICRP) [10]. In relation to the civil society and the scientific community the idea of protection against radiation starts to build up after world war two, when the effects become apparent, and were not restricted to explosions, since too many people were killed along time after the explosions, and that was due to the nuclear radiation, and radiating elements, which spread over a large area for a long time. In 1956 a public report is released by the National Academy of Science Committee stating that there is no safe threshold for radiation exposure.

After X- ray discovery, and within 3 years of that date, radiation was used in to treat cancer. At the beginning of the 20th century, shortly after that radiation began to be used for diagnosis and therapy, it was discovered that radiation could cause cancer as well as cure it (ACS 2014) [11] Even though the fatal effects became obvious in the late forties, governments around the world started to compete and run toward owning nuclear weapons, no matter what it may cause to their people and to mankind generally, for example using

simple methods of waste disposal, as it was the case of Techa river, resulted a pollution of about 100 times greater than the regular values there.

Theoretical models of radiation phenomena started to build up since its discovery. Roentgen was the first to notice the radiation reaction with air to form electricity, which is the principle behind all detector types operation, including solid material detectors. Using and invention of radiation detectors was the tool to build and support the theoretical understanding of radiation and its effects and vice versa. H. Becquerel depended on Roentgen to say that his idea applies to solids; he used the gold leaf electroscope to show that. Madame Curie depended on his work to find that the intensity of the radiation was proportional to the amount of uranium by using electroscope. In July 1898, as first step was done by J. Elster and H. Grete, and independently by C.T.R. Wilson in 1899, they had found that an electroscope steadily lost charge without apparently being exposed to radiation, they used this result to say that radioactivity is present in earth. By that time Rutherford added an important result, which was the distinction between the three known radiations alpha, beta, and gamma according to their ability of penetration (Flakus) [9].

Until 1903 instruments invented to deal with radiation were only able to see the effect of radiation or its amount. That was the case until Crooks invented the spintharoscope, which was able to detect individual rays, depending on the property of individual scintillating points of light in the zinc sulfides **screen** (Flakus) [9]. Beside this instrument was the cloud chamber invented by C.T.R. Wilson in 1911, and that still the case until A. Langsdorf upgrade the cloud chamber to diffusion cloud chamber detector with the property of being continuously sensitive, that was achieved through the thermal gradient property, which cause saturation or super saturation to the gas within the chamber. Ionizing radiation cause condensation of gas droplets representing radiation particle tracks. Now it becomes obvious to say that scientists by that time did well in trying to see the radiation individually and along a track. They used temperature and pressure gradient in gaseous emulsions, but still there is some more things required to make dependable quantitative dosimeter studies.

Scientists decided to stop using their eyes in watching the particles and counting. Making use of the progress in material science and solid state physics, it had become possible in the late forties to build Sodium Iodide doped with thallium detector. Thallium-doped sodium iodide, typically written NaI(Tl), is a scintillator that converts the energy from the incident gamma radiation into light in the visible spectrum that is then detected with a

photomultiplier tube. Properties of NaI(Tl) crystal will be understood while talking about interaction of radiation with matter in section 1.3.2, and will be discussed in the experimental set up.

Importance of radiation behavior and effects studies started to grow side by side with the wide spread of nuclear technology and its alarming consequences. As it became known, effects of nuclear technology do not consider borders between countries. As a result, countries all over the world started to study radiation levels. National institutions had been built up to deal with radiation problems; International Atomic Energy Agency (IAEA) was established on 29 July 1957, it was initiated as a growing power to guard human being against nuclear technology (IAEA) [12]. United Nations Scientific Committee on the Effects of Atomic Radiation (UNSCEAR) was established by the General Assembly of the United Nations in 1955; its mandate was to assess and report levels and effects of exposure to ionizing radiation (UNSCEAR 2000) [13]. This type of establishments didn't manage to achieve its proposed goal of promoting the peaceful and safe use of energy, but they have become a tool to help strong countries to achieve their policies mostly, where we can see the vast and unimaginable amounts of nuclear weapon everywhere. In such a realm or field, our tiny search will be nothing but lighting a candle in the series of researches done concerning measuring the radiation levels around the world and in the middle east too, this is not the first study done in Palestine, and will not be the last.

1.2 Radiation

Radiation as a phenomena was hidden until Wilhelm Roentgen's discovery of X-ray. Roentgen, a German professor of physics, was the first person to discover electromagnetic radiation in a wavelength range commonly known as X-rays today. Although, many people had observed the effects of X-ray beams before, but Roentgen was the first one to study them systematically. To highlight the unknown nature of his discovery, he called them X-rays though they are still known as Roentgen-rays as well. For his remarkable achievement he was honored with the first Nobel Prize in Physics in 1901.

Ernest Rutherford is considered the father of nuclear physics. Rutherford overturned Thomson's atom model in 1911 with his well-known gold foil experiment in which he demonstrated that the atom has a tiny, massive nucleus, which became known as the source of radioactivity.

Radiation can be classified into two main categories namely non-ionizing radiation (cannot ionize matter), and ionizing radiation (can ionize matter). The later can be divided into two types, the first is directly ionizing radiation (charged particles) such as electrons, protons, alpha particles, and heavy ions; and the second type is indirectly ionizing radiation (neutral particles) such as photons (X-rays, gamma rays), and neutrons.

Radiation is due to natural reactions that occurs in certain atoms that are unstable. The neutron–proton ratio (N/Z ratio or nuclear ratio) of an atomic nucleus is the ratio of its number of neutrons to its number of protons. Among stable nuclei and naturally-occurring nuclei, this ratio generally increases with increasing atomic number. For each element with atomic number Z small enough to occupy only the first three nuclear shells, that is up to that of calcium ($Z = 20$), there exists a stable isotope with N/Z ratio of one, with the exception of beryllium (N/Z = 1.25) and every element with odd atomic number between 9 and 19 inclusive ($N = Z+1$). Hydrogen-1 (N/Z ratio = 0) and helium-3 (N/Z ratio = 0.5) are the only stable isotopes with neutron–proton ratio under one. Uranium-238 and plutonium-244 have the highest N/Z ratios of any primordial nuclide at 1.587 and 1.596, respectively, while lead-208 has the highest N/Z ratio of any known stable isotope at 1.537. Radioactive decay generally proceeds so as to change the N/Z ratio to a new nucleus of greater stability. If the N/Z ratio is greater than 1, alpha decay increases the N/Z ratio, and hence provides a common pathway towards stability for decays involving large nuclei with too few neutrons. Positron emission and electron capture also increase the ratio, while beta minus decay will decrease the ratio.

In many cases, the instability can lead to either converting a proton to a neutron by emission of a positron and a neutrino in the so called beta plus decay, or a neutron conversion to a proton by the emission of an electron and electron antineutrino in a the so called beta minus decay.

Gamma decay may accompany other forms of decay, such as alpha and beta decays. In such cases, gamma rays are produced after the other types of decay occur. When a nucleus emits an α or β particle, the daughter nucleus is usually left in an excited state. It can then move to a lower energy state by emitting a gamma ray. Gamma decay from excited states may also follow nuclear reactions such as neutron capture, nuclear fission, or nuclear fusion.

Radiation activity is defined as the rate of nuclei decaying or disintegrating per unit time. Radiation activity of a certain nuclide in relation to any particle being emitted is a function of time. If we consider $N(t)$ particles of a radiating element under study, then the activity A will be:

$$A = -\frac{dN(t)}{dt} = \lambda N(t) \quad (1.1)$$

This has the well known solution:

$$N(t) = N_0 e^{-\lambda t} \quad (1.2)$$

where $N(t)$ here represents the remaining nuclides, and λ is the decay constant of that nuclide. This is the basic principle in dealing with the radioactive reactions.

Some parent nuclides decay to more than one daughter nuclide in parallel reactions, with each has its own probability of occurrence that leads to its own decay constant, and its total decay constant is the summation of the decay constants.

Another case is the serial decay chain, where the parent nuclide parity is 1, and the bottom of the series or the stable nuclide is $i + 1$ (with $i > 1$), nuclide 1 decays to a daughter nuclide (1 + 1), then nuclide (2) decays to its daughter (3) until reaching the stable nuclide $i + 1$, where nuclide i decay rate is considered to be λ_i . A direct application of equation (1.1) above leads to the decay rate:

$$\frac{dN_i(t)}{dt} = -\lambda_i N_i(t) + \lambda_{i-1} N_{i-1}(t) \quad (1.4)$$

This relates the last decaying nuclide rate to the parent one. Solving the above equation for two general nuclides as a parent and a daughter is enough to explain the cases of equilibrium and understand secular equilibrium, which is our tool for calculation of main NORM (Naturally Occurring Radioactive Materials) nuclides. Substituting $i = 2$, equation (1.4) becomes:

$$\frac{dN_2(t)}{dt} = -\lambda_2 N_2(t) + \lambda_1 N_1(t) \quad (1.5)$$

Applying equation (1.1), equation (1.2) to $N_1(t)$ then solving for $N_2(t)$ we get:

$$N_2 = \left(\frac{\lambda_1}{\lambda_2 - \lambda_1} \right) N_1(t=0) e^{-\lambda_1 t} + \left(N_2(t=0) - \frac{\lambda_1}{\lambda_2 - \lambda_1} N_1(t=0) \right) e^{-\lambda_2 t} \quad (1.6)$$

In some situations, the grand-daughter of a radioactive decay is still unstable and continues with producing another radioactive product. Thus, it is possible to have series or chains of radioactive decays as called ‘decay chain’ or ‘radioactive series’.

We need to talk about secular equilibrium that will be our step toward achieving the activities of the main natural chain radiation reactions of parent nuclides ^{238}U , ^{232}Th and ^{235}U .

There are three predominant cases of the state of equilibrium that can be explained as follows:

First is the case of transient equilibrium, where the half-life of the parent is longer than that of the daughter, but not significantly; $\lambda_2 > \lambda_1$. In this case we need a long time before equilibrium is attained.

Second is the case of no equilibrium where the daughter nucleus has a longer half-life than the parent one, where no equilibrium can be achieved.

Third is the case of secular equilibrium, where $\lambda_2 \gg \lambda_1$; and $\lambda_1 \cong 0$, then $e^{-\lambda_1 t}$ tends to 1, and then equation (1.6) becomes:

$$N_2 = \left(\frac{\lambda_1}{\lambda_2} \right) N_1(t=0) (1 - e^{-\lambda_2 t}) \quad (1.7)$$

After about 7 half-lives of daughter nuclide $e^{-\lambda_2 t}$ tends to zero or has no effect, this leads to:

$$\lambda_1 N_1 = \lambda_2 N_2 \quad (1.8)$$

Thus, at equilibrium, the parent and daughter activities are equal.

Figure 1.1 below demonstrates the daughter and parent nuclides activities behavior with number of daughter half lives.

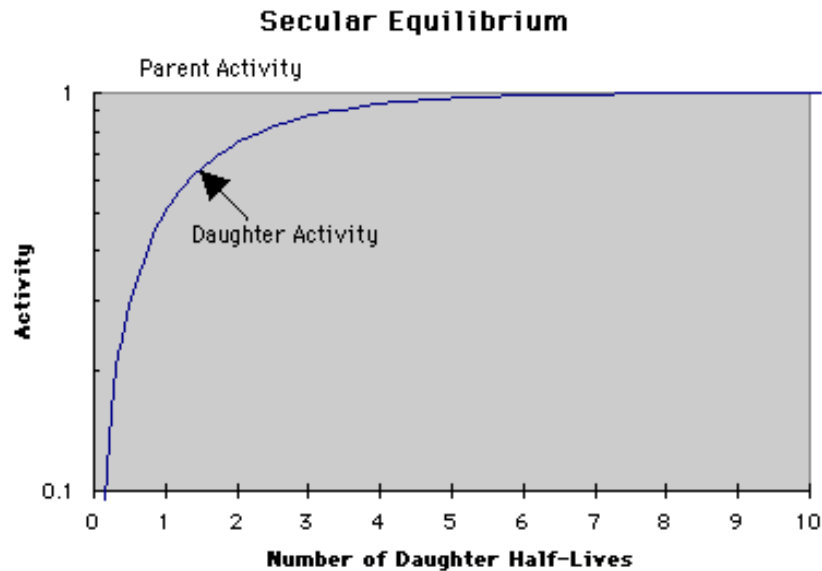


Figure 1.1 The plot of parent and daughter activity in secular equilibrium (Wagenaar 1995) [1].

If the two nuclides representing transient equilibrium or no equilibrium preceded by a grandparent nuclide having a much larger half life as it the case in ^{238}U , ^{232}Th and ^{235}U figure (1.2), (1.3) and (1.4) below, in this case, secular equilibrium is achieved, and each one's activity will be representing the dominating activity of the grandparent nucleus.

If we look at ^{238}U chain decay, it is obvious depending on the above notes, and figure (1.2) shown below that ^{234}Pa and ^{234}U are supposed to be in no equilibrium, but with ^{238}U domination, each is in secular equilibrium with ^{238}U , and for ^{234}U and ^{230}Th they are in transient equilibrium, but with ^{238}U domination, both are in secular equilibrium with ^{238}U , this applies all the way down to ^{206}Po , and all could be used as representatives to ^{238}U activity. In the case of ^{232}Th and ^{235}U in radioactive chains shown in figure (1.3) and figure (1.4) below, same thing applies as the ^{238}U series.

In theory, secular isotopic equilibrium is attained in uranium deposits after approximately 1.7 million years if mineralization behaves as a closed geochemical system. This theoretical result assumes introduction of ^{238}U as the only uranium isotope (Stratamodel 2016) [14]. Thus extracting the soil samples is supposed to be done by digging an ironic

cylindrical shell, or in other words you have to do that like cutting a piece of cheese without any fallings. With such hypothesis we can use any of chains nuclides as a representative to the parent nuclide activity, assuming that the samples destinations are closed geochemical systems.

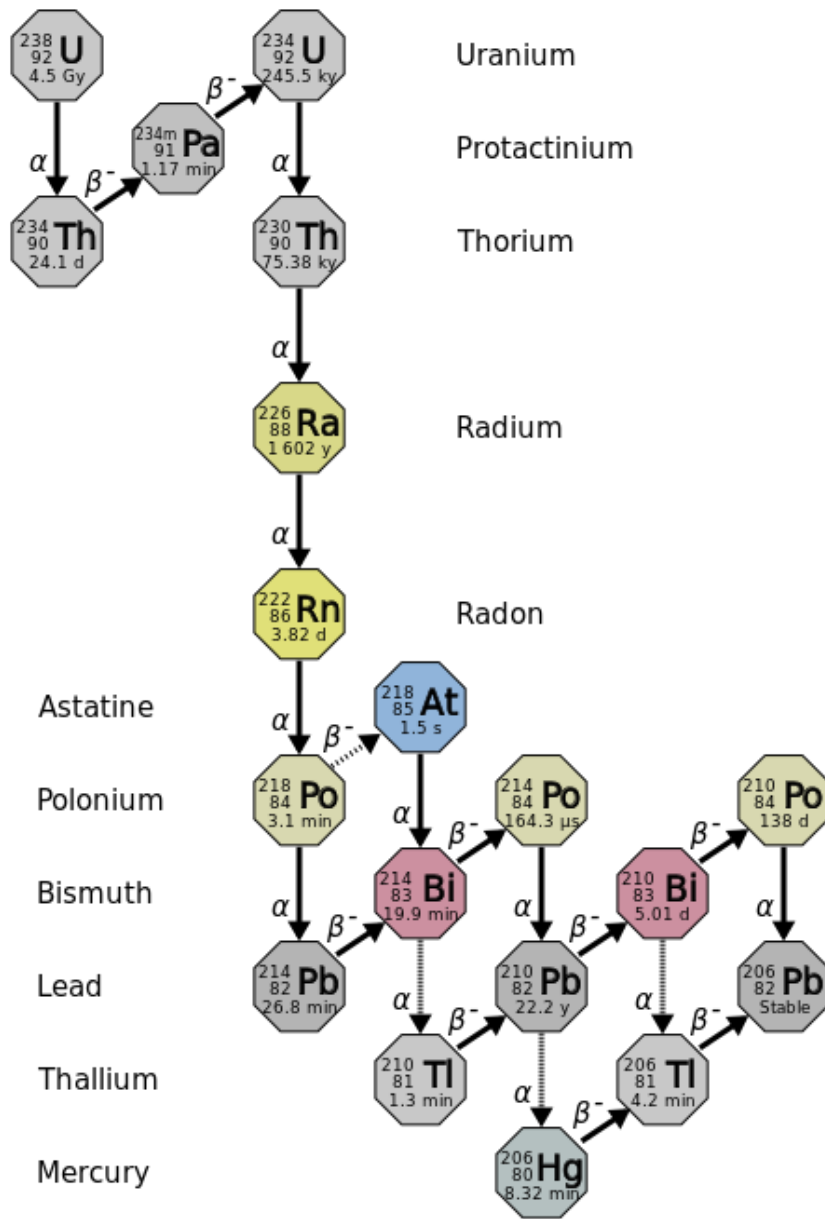


Figure 1. 2: U-238 decay chain series (Commons 2015) [15].

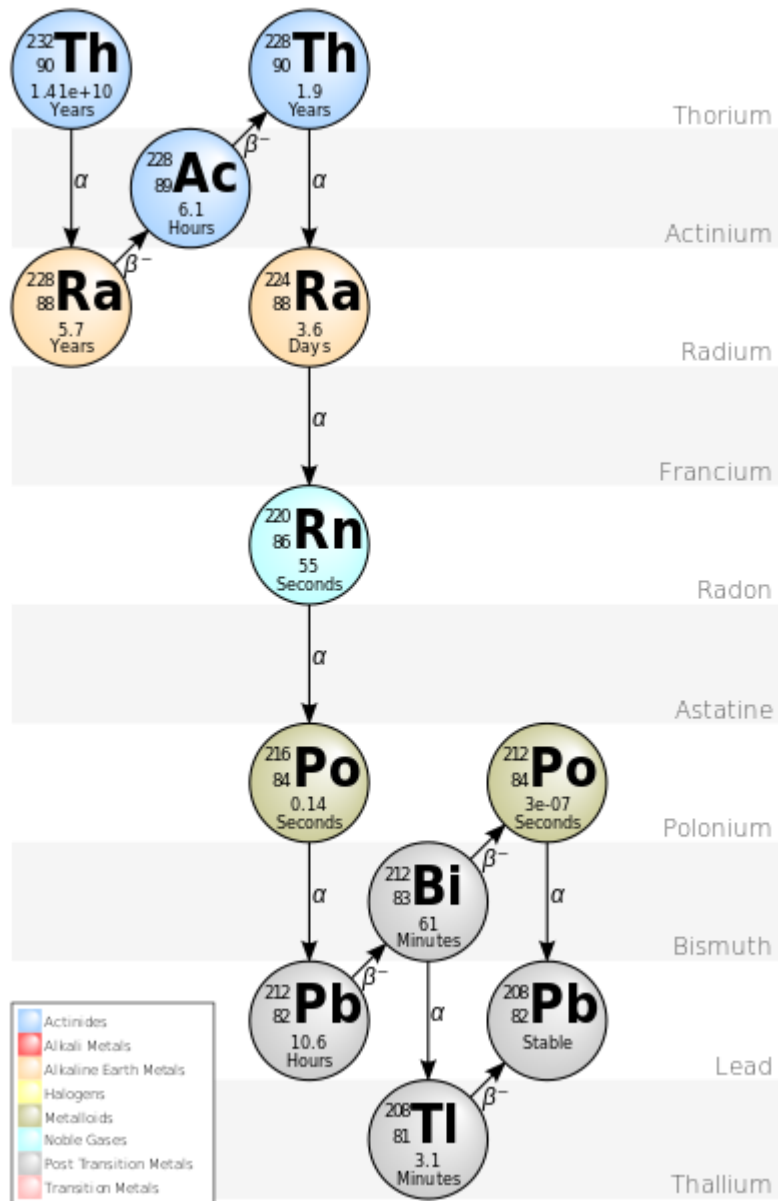


Figure 1.3: Th-232 decay chain series (Commons 2015) [16].

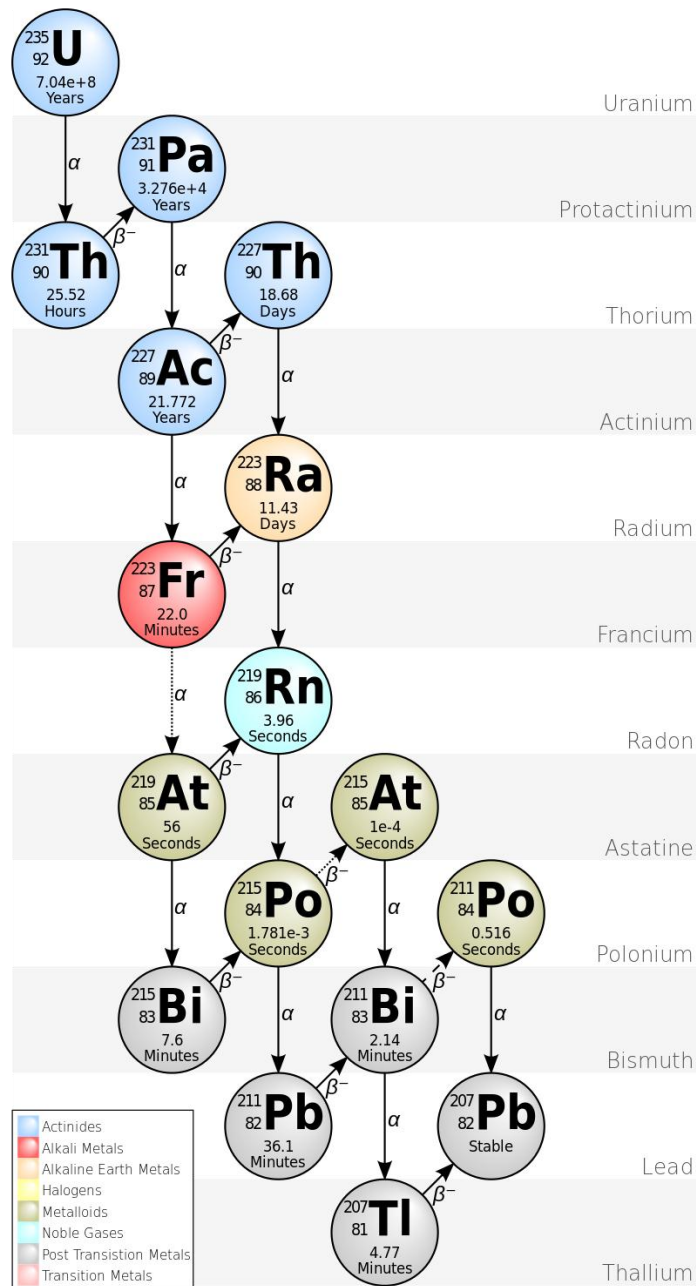


Figure 1. 4: U-235 decay chain series (Wikipedia 2008) [17].

1.3 Gamma radiation

This kind of radiation contains high quanta of energy that ranges from a few keV to more than 100 MeV. With this amount of energy that gamma rays have, it is an ionizing electromagnetic wave, it also can penetrate the atomic space and collide with the nucleus to form the phenomena of pair production, it could even form pair production in the vicinity of atomic particles potential fields. Also it can penetrate through human body without any interaction.

1.3.1 Theory behind gamma ray phenomena

In the above paragraphs we did talk about the resulting nuclear radiation behavior. The deep view behind that could be understood through studying of the nuclear electromagnetic fields in an integrated view.

It is known classically that the nucleus is being considered as a distribution of non static charge in which we have electric and magnetic multi-pole effects, where this multi-pole effect considered is dependent upon our level of approximation in dealing with the nucleus electromagnetic field behavior, which is dependent on how distant the point we are measuring that effect at (Reitz, Milford et al. 1993) [18]. The approximation is also dependent on the kind of experimental results people used to experience in dealing with the measured nuclear radiation. Solving the electromagnetic problem for this nuclear distribution of charge, with charges considered in reactive motion or non static in the form of antennas with dimensions comparable to wavelength (Jackson 1999) [19] and keeping the multi-pole terms in solving for electric and magnetic fields, then solving for the radiated power of electric or magnetic field, we get the following general form as it is adopted by (Dokhane 2007) [20]:

$$P(\sigma L) = \frac{2(L+1)c}{\varepsilon_0 L [(2L+1)!!]^2} \left(\frac{\omega}{C}\right)^{2L+2} [m(\sigma L)]^2 \quad (1.9)$$

P is the power radiated, L is the angular momentum, ω is the angular frequency of the radiation, σ represents the field either electric or magnetic, ε_0 is the permittivity of free space, $m(\sigma L)$ is the amplitude of the electric or magnetic multi-pole moment.

Moving to quantum mechanics, where the radiation is quantized into photons of energy $E = h\nu = \hbar\omega$ (Cohen 1971) [21] then the rate of emission of photons is:

$$\lambda(\sigma L) = \frac{P(\sigma L)}{\hbar\omega} \quad (1.10)$$

With eq(1.9) we get:

$$\lambda(\sigma L) = \frac{2(L+1)c}{\varepsilon_0 \hbar L [(2L+1)!!]^2} \left(\frac{\omega}{C}\right)^{2L+1} [m(\sigma L)]^2 \quad (1.11)$$

In quantum representation the multi-pole moment $m(\sigma L)$ amplitude is exchanged into an operator constituting an (f i; with i stands for initial and f stands for final) element matrix according to the following form:

$$m_{fi}(\sigma L) = \int \Psi_f^* m(\sigma L) \Psi_i d\nu \quad (1.12)$$

where Ψ_f is the final state of the nucleus, Ψ_i is the initial state of the nucleus, integration is done over the nucleus volume, $m(\sigma L)$ operates on the nucleus initial state to change it to Ψ_f . According to Weisskopf estimate as shown in (Dokhane 2007) [20] of a single proton shell model of EL and ML, transitions probability become:

$$\lambda(EL) = \frac{2(L+1)c}{\varepsilon_0 \hbar L [(2L+1)!!]^2} \left(\frac{\omega}{C}\right)^{2L+1} \frac{e^2}{4\pi} \left(3 \frac{R^L}{L+3}\right)^2 \quad (1.13)$$

$$\lambda(ML) = \frac{2(L+1)c}{\varepsilon_0 \hbar L [(2L+1)!!]^2} \left(\frac{\omega}{C}\right)^{2L+1} 10 \left(\frac{\hbar}{m_p c R}\right)^2 \frac{e^2}{4\pi} \left(3 \frac{R^L}{L+3}\right)^2 \quad (1.14)$$

With R as the nuclear radius ($R_0 A^{1/3}$), m_p is the proton mass.

1.3.1.1 Selection rules

There are several quantized possibilities of emissions that we can think of according to angular momentum L operator in equation (1.12) and considering Ψ_i to have angular momentum I_i and Ψ_f to have I_f . To satisfy conservation of angular momentum, the following vector triangle is supposed to be satisfied:

$$|I_i - I_f| \leq L \leq |I_i + I_f| \quad (1.15)$$

Where this is equivalent to a result of 2^L possible multi-pole orders, according to the index or operator values L. Also L is not allowed to have a zero value, since that means the initial and final energy states are equal, with a difference of zero, and no radiation occur. For example in a quadruple approximation, L has a value of two, which means we have four values for λ .

One more variable need to be considered is the parity, which is the sign change of the radiation field as a result of axis reflection and is related to L operator, to explain that we

need to consider an example in which $I_i = 3/2$ and $I_f = 5/2$, then L have the values 1, 2, 3, 4.

$$\pi(ML) = (-1)^{L+1} \quad (1.16)$$

$$\pi(EL) = (-1)^L \quad (1.17)$$

where π represents the parity, these two equations or restrictions above are no more than a summary of the results of sign behavior of the initial and final state wave functions under reflection of axis. In other word, for cases of no change in parity you can use the equations (1.16) and (1.17) to say that L=1, 3 in the above example are due to the magnetic dipole and octupole, and side by side L=2, 4 are due to electric Quadra-pole and hexadeca-pole. But if we have a change in parity then the opposite of the above is the case.

It is true that in our study we will be trying to make sample analysis to determine its elements depending on radioactivity measurements, but this is just a little part of the effort of others who did bridge the gap between experimental radioactivity measurements and building a dependable theoretical model for interpretation as we discussed above. On the other hand our spectrum analysis peaks was the tool to build isotopes library energies and the probabilistic appearance of the peaks, and recommendation of nuclear models.

1.3.2 Gamma radiation interaction with matter

Gamma rays have no charge, but it has relatively great amount of energy. This means that its probability of interaction with atomic electrons is a lot smaller than that of alpha radiation for example, or in otherwords it could be said that gamma ray cross-section of interaction is a lot less than beta and alpha interactions. The high energy of gamma rays is the reason behind its ability of penetration.

Gamma ray interaction with matter has several possibilities that all constitute the photon interaction cross-section with an atom (Ragheb) [22]. The most important of these are the following:

1.3.2.1 Photoelectric effect

First is the photoelectric effect, in which the photon is absorbed totally by the emitted electron, the recoiling atom, and the emitted electron to pass over its binding energy. In symbol form, consider E_γ being the gamma photon energy, E_e being electron energy, E_a as the energy attained by the recoiling atom, which is of the order of 10^{-4} relative to the recoiling electron energy, and is ignored. The binding energy of the electron, which is found to be a k shell electron, considered as E_b is :

$$E_b = 13.6(Z - 1)^2 eV \quad (1.18)$$

With Z as the atomic number. The ejected electron energy is:

$$E_e = h\nu - E_b \quad (1.19)$$

Substituting for E_b we get

$$E_e = h\nu - 13.6(Z - 1)^2 eV \quad (1.20)$$

where E_γ is $h\nu$ with h as Planck's constant, and ν is the photon frequency. This result explains the photoelectric interaction if it occurs.

Electrons resulting from photoelectric effect have to be replaced by electrons from higher levels with the emission of photons representing the difference in energy forming a characteristic spectrum of light representing the scintillation material; these photons are in the X-ray level of energy, called fluorescent X-rays. The ejected electron is called a photoelectron and is usually considered a secondary electron or a secondary beta emission. Such electrons can produce what is called bremsstrahlung X-rays, which is ionizing too (Serman) [23].

Cross-section of interaction is related to the study of shielding against radiation, and to the study and choice and building of scintillation materials. It is shown that the photoelectric interaction cross-section is inversely proportional to the gamma photon energy and is directly proportional to the atomic number Z as follows:

$$\sigma_{pe} = \frac{cZ^n}{(h\nu)^m} \quad (1.22)$$

where m ranges from 1 to 3 and n ranges from 4 to 5 (Ragheb) [22].

1.3.2.2 Compton scattering

In Compton scattering a photon scatters from an atomic electron usually considered at rest.

The electron leaves the atom in what is considered elastic scattering as shown in figure 1.5 below. Scattered photon inturn could go into either more Compton scattering or it could vanish in aphotoelectric interaction. Employing conservation of energy and momentum in the relativistic manner, with E'_γ is the energy of the scattered photon, E_γ is the energy of the incident photon, E_0 is the rest mass energy of the electron, and θ is the angle between the direction of the incident and scattered photons, we can arrive to the following equation:

$$\frac{1}{E'_\gamma} - \frac{1}{E_\gamma} = \frac{1 - \cos \theta}{E_0} \quad (1.23)$$

where $E_0 = m_0c^2$, $E'_\gamma = hv'$, $E_\gamma = hv$, then rearranging the equation above one gets:

$$hv' = \frac{hv}{1 + \frac{hv}{m_0c^2}(1 - \cos \theta)} \quad (1.24)$$

Energy of the electron representing the Compton continuum is"

$$E_e = hv - hv' \quad (1.25)$$

Substituting for hv' from equation (1.24) into equation (1.25) we get (Knoll 2010) [24]:

$$E_e = \frac{\frac{hv}{m_0c^2}(1 - \cos \theta)}{1 + \frac{hv}{m_0c^2}(1 - \cos \theta)} \quad (1.26)$$

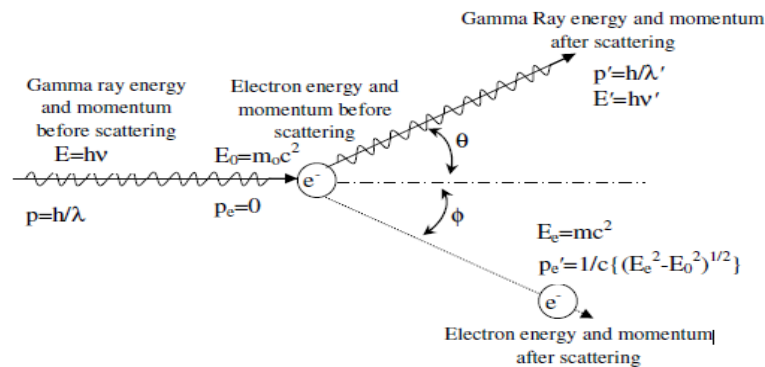


Figure 1.5: Schematic diagram of Compton Effect kinematics (Parks 2015) [2].

One more point need to be said is that electrons resulting in Compton scattering could also produce bremsstrahlung X-rays.

The Compton Effect cross-section is proportional to the atomic number Z :

$$\sigma_c \approx \text{constant} \cdot Z \quad (1.27)$$

1.3.2.3 Pair production

Pair production is the creation of an elementary particle and its antiparticle, for example creating an electron and positron, a muon and antimuon, or a proton and antiproton. Pair production often refers specifically to a photon creating an electron-positron pair near a nucleus but can more generally refer to any neutral boson creating a particle - antiparticle pair. In order for pair production to occur, the incoming energy of the interaction must be above a threshold in order to create the pair – at least the total rest mass energy of the two particles – and that the situation allows both energy and momentum to be conserved. However, all other conserved quantum numbers (angular momentum, electric charge, lepton number) of the produced particles must sum to zero – thus the created particles shall have opposite values of each other. For instance, if one particle has electric charge of +1 the other must have electric charge of -1, or if one particle has strangeness of +1 then another one must have strangeness of -1. The probability of pair production in photon-matter interactions increases with photon energy and also increases approximately as the square of atomic number of the nearby atom.. The pair production cross section increases with increasing atomic number Z as:

$$\sigma_{pp} \approx \text{constact} \cdot Z^2 \quad (1.28)$$

1.3.2.4 Fluorescent X-ray

X-ray fluorescence (XRF) is the emission of characteristic "secondary" (or fluorescent) X-ray from a material that has been excited by bombarding with high-energy X-rays or gamma rays. This term is generated in Compton scattering and photoelectric effect reactions, and shows may show up in the acquired spectrum. In this case it may appear as a separate peak.

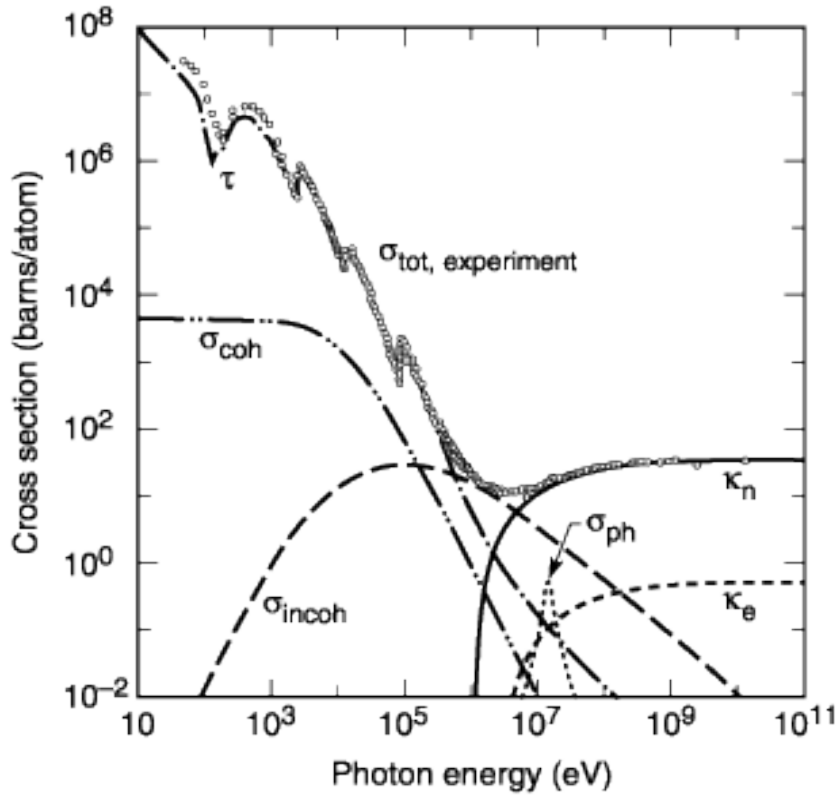


Figure 1.6: Total photon cross section in lead as a function of energy (Kirz) [3].

Figure 1.6 above demonstrates all contributions of gamma ray cross-section of interaction in lead as a function of energy. In the figure, τ represents photoelectric effect, σ_{coh} represents Rayleigh scattering, σ_{incoh} represents Compton scattering, σ_{ph} represents photonuclear absorption, k_n represents nuclear field pair production, k_e represents electron field pair production

1.4 Radiation Dosimetry

In scope of the theoretical discussion given above about interaction between radiation and matter we can build up our measurement system, and the technologies concerning that. On the other hand, below we will discuss the key quantities that demonstrate our measured value, which is the activity.

1.4.1 Activity

Activity could be defined as the number of atoms of a certain source that decay and emit radiation in one second as in equation (1.1) above. For a certain source that is a mixture containing one radioactive material or more, our peak position on the spectrum will be the road to guess what kind of isotopes we have, and using the count number at the peak we can calculate the concentration activities and percent weight of these materials in the mixture. The average number of decays per second in the International System (SI) unit for activity is the Becquerel (Bq), which is that quantity of radioactive material in which one atom transforms per second (NDT) [6].

1.4.2 Intensity

The other interesting and important value that our system will be measuring to be able to determine activity is the intensity which is defined as the amount of energy or radiation passing through a given area that is perpendicular to the direction of radiation travel in a given unit of time (NDT) [6].

Translating that to a mathematical equation, consider the point source in figure 1.7 with an N number of gamma rays being emitted per second isotropically, and the 2*2 NaI(Tl) detector as shown in the same figure below, by building a gaussian surface with a radius r from the source to the circular edge of the cylindrical detector, the source intensity will be:

$$I_{source} = \frac{N}{4\pi r^2} \quad (1.29)$$

The counts received by the detector come through the sphere cap shown or the front circular surface of the crystal detector, then the maximum intensity received by the crystal detector is:

$$I_{detector} = I_{source} * \frac{Cap\ area}{sphere\ area} \quad (1.30)$$

then

$$I_{detector} = \frac{N(Rh_c)}{8\pi r^4} \quad (1.31)$$

where h_c is the cap height

Then the geometrical efficiency is

$$\mathcal{E}_g = \frac{I_{detector}}{I_{source}} \quad (1.31)$$

Which gives

$$\mathcal{E}_g = \frac{Rh_c}{2r^2} \quad (1.32)$$

This is just a hypothetical explanatory system with the source considered as a point source, where it is not as could be seen with our samples taking the cylindrical plastic mernalli shape, and isotropy is hypothetical too, where that need to be shown, and it is a matter of study.

We need now to calculate the intrinsic efficiency of the detector crystal, which relates to gamma ray interaction with matter as discussed in section 1.3.2

$$\mathcal{E}_{int} = \frac{I_{cathode}}{I_{detector}} = \frac{\int_0^{\theta_1} [1-e^{-\mu(E)[\frac{L}{\cos\theta}]}] \sin\theta d\theta}{[1-\cos\theta_0]} + \frac{\int_{\theta_1}^{\theta_0} [1-e^{-\mu(E)[\frac{L}{\sin\theta} - \frac{d}{\cos\theta}]}] \sin\theta d\theta}{[1-\cos\theta_0]} \quad (1.33)$$

Where $\tan\theta_0 = \frac{R}{d}$, $\tan\theta_1 = \frac{R}{d+L}$, $\mu(E)$ is the linear attenuation coefficient in NaI(Tl) for photon with energy E, and $I_{cathode}$ is the radiation pieces intensity at the photocathode shown in the figure below.

Last you need to consider the photocathode efficiency since not all radiation reaching it get translate to the photomultiplier tube but about 15% of that, then:

$$\mathcal{E}_{tot} = \mathcal{E}_g * \mathcal{E}_{int} * \mathcal{E}_{cathode} \quad (1.35)$$

Then

$$\mathcal{E}_{tot} = \frac{Rh_c}{2r^2} * \left[\frac{\int_0^{\theta_1} [1-e^{-\mu(E)[\frac{L}{\cos\theta}]}] \sin\theta d\theta}{[1-\cos\theta_0]} + \frac{\int_{\theta_1}^{\theta_0} [1-e^{-\mu(E)[\frac{L}{\sin\theta} - \frac{d}{\cos\theta}]}] \sin\theta d\theta}{[1-\cos\theta_0]} \right] * \mathcal{E}_{cathode} \quad (1.34)$$

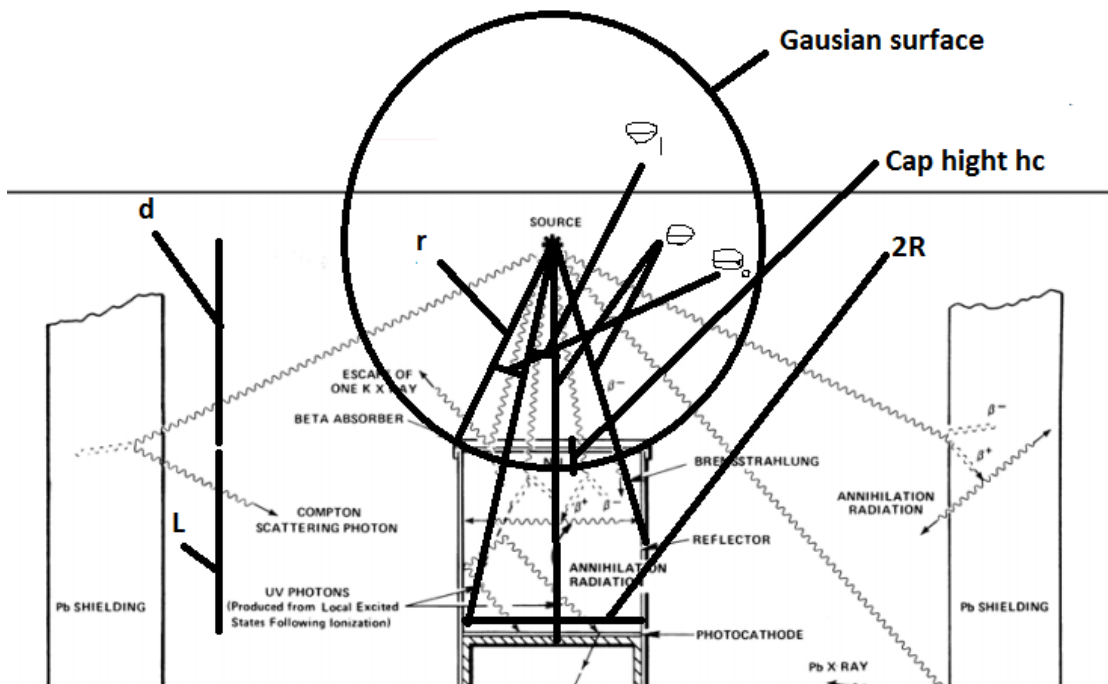


Figure 1.7: Intensity manipulation across 905-3 NaI(Tl)

The importance of this value over activity, is that it is hard to measure the activity directly without taking into consideration the geometry of the detector. Measurement of the intensity is then related to the activity we need to solve for.

1.4.3 Exposure

Third quantity is the exposure that could be defined as the level or extent to which a unit mass of air could get ionized by a certain radiating source. Its unit of measurement is the roentgen (R) named after the well known scientist Roentgen. A Roentgen is the amount of photon energy required to produce 1.610×10^{12} ion pairs in one gram of dry air at 0°C . A radiation field of one Roentgen will deposit 2.58×10^{-4} coulombs of charge in one kilogram of dry air (NDT) [6], Since we trying to assess the hazardous effect of naturally occurring radiation, a special case of exposure is required which is external exposure at 1 meter above the ground level that is due to terrestrial radionuclides present in our sample.

1.4.4 Absorbed dose, dose equivalent, and dose rate

Another three important quantities we will consider here are the absorbed dose, dose equivalent, and dose rate. Absorbed dose is the amount of energy that ionizing radiation

imparts to a given mass of matter. In other words, the dose is the amount of radiation absorbed by and object. The SI unit for absorbed dose is the gray (Gy), but the “rad” (Radiation Absorbed Dose) is commonly used. 1 rad is equivalent to 0.01 Gy. Different materials that receive the same exposure may not absorb the same amount of radiation. In human tissue, one Roentgen of gamma radiation exposure results in about one rad of absorbed dose. The dose equivalent relates the absorbed dose to the biological effect of that dose. The absorbed dose of specific types of radiation is multiplied by a "quality factor" to arrive at the dose equivalent. The SI unit is the sievert (SV), but the rem is commonly used. Rem is an acronym for "roentgen equivalent in man." One rem is equivalent to 0.01 SV. When exposed to X- or Gamma radiation, the quality factor is 1. Finally, Dose Rate: The dose rate is a measure of how fast a radiation dose is being received. Dose rate is usually presented in terms of R/hour, mR/hour, rem/hour, mrem/hour (NDT) [6].

1.5 Biological Effects of Radiation

Biological effects of radiation is a major subject. However, very briefly, biological effects of radiation are typically divided into two categories. The first category consists of exposure to high doses of radiation over short periods of time producing acute or short term effects. The second category represents exposure to low doses of radiation over an extended period of time producing chronic or long term effects. High doses tend to kill cells, while low doses tend to damage or change them. High doses can kill so many cells that tissues and organs are damaged. This in turn may cause a rapid whole body response often called the Acute Radiation Syndrome (ARS). Low doses spread out over long periods of time don't cause an immediate problem to any body organ. The effects of low doses of radiation occur at the level of the cell, and the results may not be observed for many years.

If radiation interacts with the atoms of the DNA molecule, or some other cellular component critical to the survival of the cell, it is referred to as a direct effect. Such an interaction may affect the ability of the cell to reproduce and, thus, survive. If enough atoms are affected such that the chromosomes do not replicate properly, or if there is significant alteration in the information carried by the DNA molecule, then the cell may be destroyed by “direct” interference with its life-sustaining system.

1.6 Gamma ray and medication

The property of causing death of cells by radiation, including gamma rays, that showed up to scientists around the time radiation was discovered, was the same property that made it emerge as a tool for curing the damage it makes. By that time, curing cancer was limited to the old techniques of surgery and burning of tumor. Burning as an old clinical technique led scientist to using photon therapy (X ray and gamma ray). Cure with radiation differs from one type of radiation to the other and from one tissue to the other. Photon Therapy is by far the most common form of radiation used for cancer treatment. It is the same type of radiation that is used in x-ray machines, and comes from a radioactive source such as cobalt, cesium, or a machine called a linear accelerator (linac, for short). Photon beams of energy affect the cells along their path as they go through the body to get to the cancer, pass through the cancer, and then exit the body. Some published reports suggest that the statistical results of photon therapy is bad enough to the level that staying without a cure is even better in most of the cases (Cure) [25].

Neutron therapy has two branches: Fast Neutron Therapy (FNT) and Boron Neutron Capture Therapy (BNCT). The mean neutron energies used for FNT range from 2 MeV to 25 MeV whereas the maximum energy for BNCT is about 10 keV. Neutron generators for FNT have been cyclotrons, accelerators and reactors, whereas BNCT is so far bound to reactors. Both therapies use the effects of high-LET radiation (secondary recoil protons and alpha particles, respectively) and can attack otherwise radio resistant tumours, however, with the hazard of adverse effects for irradiated healthy tissue.

Boron neutron capture therapy (BNCT) was recognized as a potential technique in treating cancer by the time the neutron was discovered in 1932. And up to this day it is showing up as one of the greatest tools, especially when it comes to dealing with tissues that are close to sensitive places like the eye or the brain, where we are supposed to minimize the effect on normal neighboring tissues. The idea in this process is to inject the tumor with the nonradioactive boron to prepare it to capture the neutron beam particles according to the following nuclear reaction in (Barth, Vicente et al. 2012) [26]:



Briefly speaking the results of this reaction are helium and lithium that are energetic with about 2.79 MeV of kinetic energy. These particles have a combined range in tissue of 12–

13 μm (comparable to cellular dimensions). In other words the reaction designed to kill the cancer cell will happen approximately within the dimensions of that cell, and that is the guarantee for safety of the healthy cells.

3D-dose calculation systems have been developed at several facilities and guarantee a high safety for both therapies, FNT and BNCT.

Carbon ion radiation can be helpful in treating cancers that don't usually respond well to radiation (called radioresistant). It's also called heavy ion radiation because it uses a particle that's heavier than a proton or neutron. The particle is part of the carbon atom, which itself contains protons, neutrons, and electrons. Because it's so heavy, it can do more damage to the target cell than other types of radiation. As with protons, the beam of carbon ions can be adjusted to do the most damage to the cancer cells at the end of its path. But the effects on nearby normal tissue can be more severe. This type of radiation is only available in a few centers in the world.

Conformal proton beam is another technique to compare with X and gamma ray, it took advantage of the proton property of high cross section of interaction, which made the localization of the reaction possible, another property achievable with proton beam usage is the depth at which the reaction happen, where this can be done by regulating the velocity of the beam.

Proton beam uses a similar approach of X and gamma ray in focusing radiation on the cancer. This means that proton beam radiation can deliver more radiation to the cancer while possibly reducing damage to nearby normal tissues [27].

1.7 Study motivations

Human have a tendency toward exploring nature, the motives behind that are: achieving safety, facilitating life, and enjoying the discovery and understanding of the unseen. These were the reasons behind the emergence of radiation as a branch of study. Bad or fatal effects of radiation contradict safety. Using of radiation for medical purposes helps in achieving safety too.

Study of radioactivity levels is being done all over the world. The reason for that is to determine the level of natural radiation that differs from one place to the other according to

the earth geography and features. On the other hand, we have the artificial radiating materials that have been distributed all over the world through many means, one is the waste disposal. Second could be the rain that is able to capture and transfer radiating material, artificial and natural, and spread it all over the world. Third could be the using of radiating materials in weapons and spreading it accompanying wares.

1.7 Previous studies in Palestine

Few studies on natural radioactivity concentration measurements are reported. Here are some of the well known studies conducted in the West Bank- Palestine.

1. Natural Alpha Particle Radioactivity In Soil In Hebron (Hasan 1999) [28].
2. Assessment of Natural and Man–Made Radioactivity Levels of the Plant Leaves Samples as Bio- Indicators of Pollution in Hebron District- Palestine (Dabayneh 2006) [29].
3. Radioactivity Levels in Some Plant Samples in the North Western of West - Bank , Palestine and Evaluation of the Radiation Hazard (Thabayneh and Jazzar 2013) [30].
4. Radioactivity Measurements in Different Types of Fabricated Building Materials used in Palestine (Dabayneh 2007) [31].
5. Environmental Nuclear Studies of Natural and Manmade Radioactivity at Hebron Region in Palestine (Dabayneh, Sroor et al. 2008) [32].
6. Natural Radioactivity in Different Commercial Ceramic Samples Used in Palestinian Buildings as Construction Materials (Dabayneh 2008) [33].
7. Radioactivity Concentration in Soil Samples in the Southern Part of the West Bank- Palestine (Dabayneh, Mashal et al. 2008) [34].
8. Natural Radioactivity Levels and Estimation of Radiation Exposure in Environmental Soil Samples from Tulkarem Province – Palestine (Thabayneh and Jazzar 2012) [35].
9. Determination of Natural Radioactivity Concentrations and Dose Assessment in Natural Water Resources from Hebron Province, Palestine(Thabayneh, Abu-Samreh et al. 2012) [36].
10. Measurement of Natural Radioactivity and Radon Exhalation rate in Granite samples Used in Palestinian Buildings (Thabayneh 2013) [37].
11. Transfer of Natural Radionuclides from Soil to Plants and Grass in the Western North of West Bank Environment- Palestine (Jazzar and Thabayneh 2014) [38].

12. Measurement of Radioactivity Concentration Levels of Natural Radionuclides in Soil Samples from Bethlehem Region – Palestine (ABU SAMREH, THABAYNEH et al. 2014) [39].
13. Soil-to-Plant Transfer Factors and Distribution Coefficient of ^{137}Cs in Some Palestinian Agricultural Areas (Thabayneh 2015) [40].
14. Determination of Alpha Particles Concentration in Some Soil Samples and the Extent of their Impact on the Health (Thabayneh 2016) [41].
15. Radionuclides Measurements in Some Rock Samples Collected from the Environs of Hebron Region –Palestine (Thabayneh, Mashal et al. 2016) [42].

Chapter Two
Experimental Equipments and Procedures

Chapter Two

Experimental Equipments and Procedures

2.1 Introduction

The experimental tools employed toward our results are mainly: the soil samples and its collection destinations to be proper and representative, and its preparation to conform the scientific criteria that are being followed around the world to avoid misleading and errors. Second is the detection and manipulation system up to the creation of the spectrum and its analysis for its contents of isotopes.

2.2 Samples and the Destinations of collection

Studies have been done along the west bank of Jordan River by a number of Palestinian scientific teams, and under more than one title concerning the type of radiating elements being searched for, and on the other hand the exposed positions or situations, like buildings and their materials. In this study we chose to collect soil samples from southern villages of Hebron governorate given the symbols a_i , and villages in the north of Hebron given the symbols b_i , then villages in south of Bethlehem given the symbols c_i as shown in figures 2.1, 2.2, 2.3, 2.4 below.

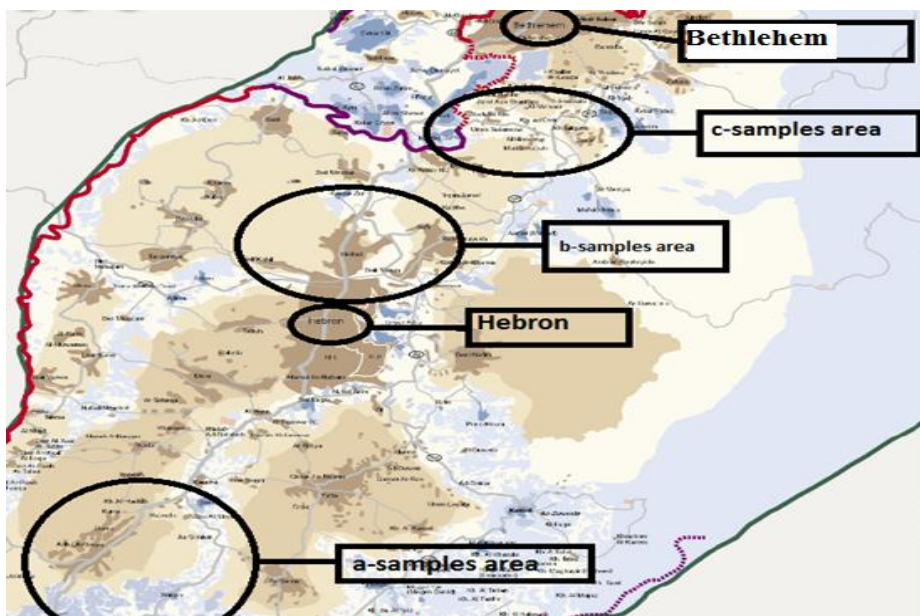


Figure 2.1: The three main areas of study circled and named.



Figure 2.2: Destinations of collection of samples c1 through c4 circled as shown.



Figure 2.3: Destinations of collection of samples b1 through b4 circled as shown.

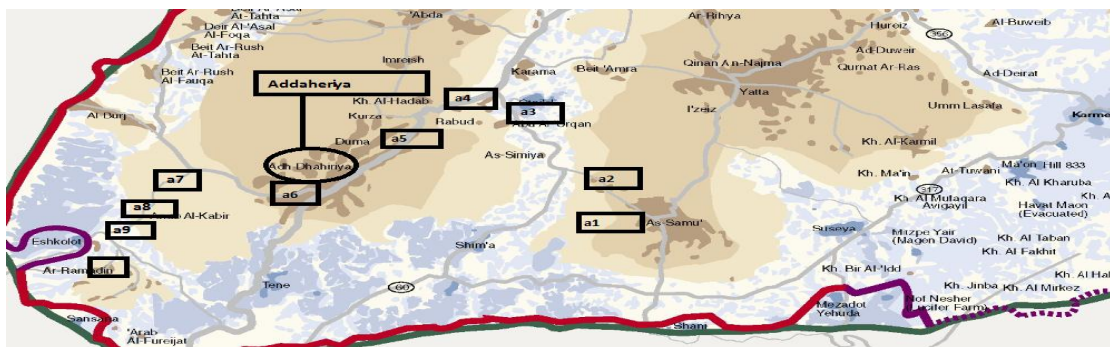


Figure 2.4: Destinations of collection of samples a1 through 10 circled as shown.

All the 4 maps are offered by (World map finder web site) [43].

We started collecting the first 10 samples along the east to west direction starting by middle of Assamu' town up till Arramaden village next to Addaheriya town. The second group, consists of 4 samples, were collected starting by Ayn Sa'eer in Sa'eer town and

ending up at the far west of Halhul town. Last group, consists of 4 samples, were collected starting by a sample around the centre of Tuqu' up till the Asioon village. We tried to make the samples equally distributed along each of the west to east lines. We tried to go as deep as 40 centimeter to avoid any substance that could be due to cultivation and pollution. Also we avoided stones to achieve the symmetry of the samples. Then at that level of 40 centemere, considered as the zero level, we collected each sample according to the template method dimentions The samples was grinded such that we can get 500 gram samples with the property of its granules being able to pass through the two by two millimeter bolter or screen, during grinding we used to spread the samples in sun light for about 15 days so that we can get approximately the same level of moisture in all samples up to the moment of baking them up in the nylon bags. It becomes now ready for measurement.

2.3 Experimental setup

The experimental set up shown in Figure 2.2 below will be used to collect our spectrum. This system is constituted of:

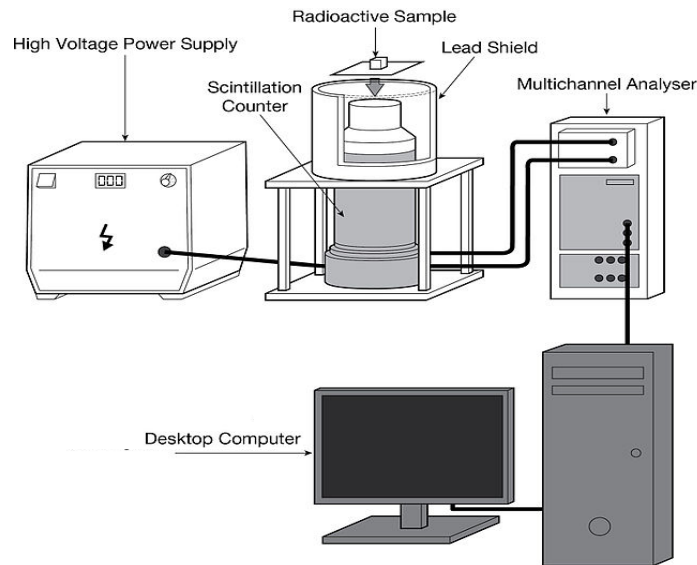


Figure 2.5: A typical experimental setup for determination of γ -radiation spectrum

2.3.1 905-3 NaI(Tl) Scintillation Detector

In Figure 2.6 below we can see the 905-3 NaI(Tl) parts:

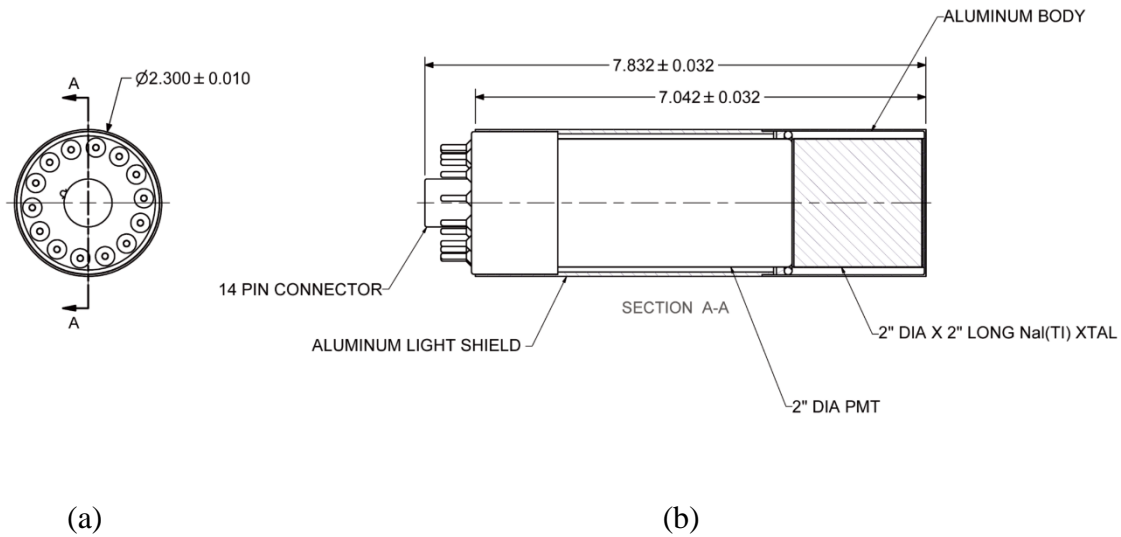


Figure 2.6: (a) The fourteen pin connector of the 905-3 NaI(Tl). (b) 905-3 NaI(Tl) (ORTEC®) [4].

Part (a) on right of Figure 2.6 is a fourteen pin connector that supplies PMT's circuit with the high voltage as shown in Figure 2.7 below:

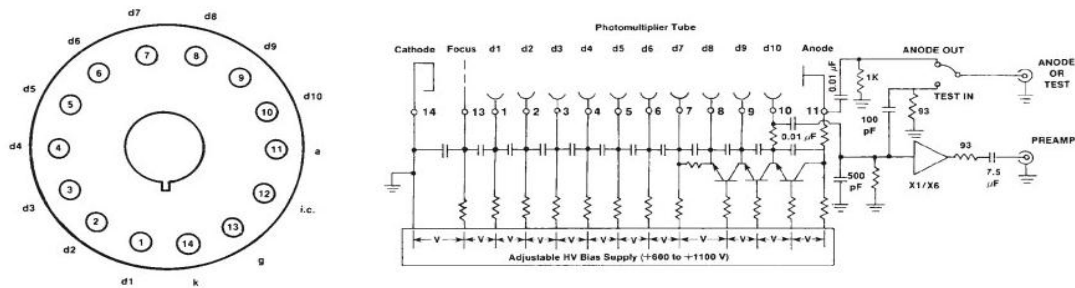


Figure 2.7: Electrical circuit design of the fourteen pinconnector, they connects to the cathode and anodes within the PMT (ORTEC®) [4].

In part b of Figure 2.6, the NaI(Tl) crystal can be seen in the far left, covered by an aluminum body. In the middle we can see the PMT shielded with a thin layer of aluminum, dimensions of the 905-3 NaI (Tl) is shown with "DIA" stands for diameter. NaI is an alkali halide inorganic scintillator with a relatively high Z from iodine (53), this type of detecting or scintillating material crystal has good and required properties; among these is the relatively high efficiency as shown in Figure 2.8 below:

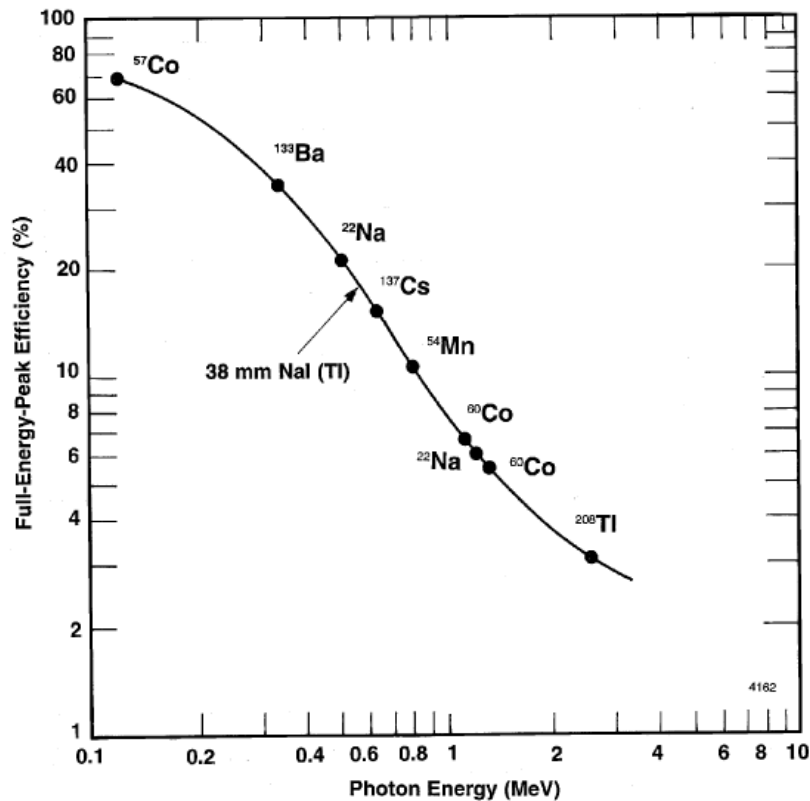


Figure 2.8: Detecting material Efficiency as a Function of Energy.

NaI(Tl)'S efficiency is related to the high Z number of iodine, on the other hand it is related to the activating material of thallium that has the important properties of improving sensitivity that leads to better efficiency, It possesses well-characterized emission bands and has a very short emission lifetime of (10^{-6} – 10^{-7}) s (ALDRICH) [44].

The other important property of **NaI (TI)** is resolution, which is the ability of the scintillating crystal to separate the peaks (decrease their overlap in the resulting spectrum). Resolution of the scintillating material is dependent on the light decay time constant. In **NaI (TI)** crystal; using pure NaI we get a light decay time constant of 60 ns, but when thallium is doped the decay time increase to 230 ns which leads to a decrease in resolution, in this case we can notice the exchange high resolution with a lot of efficiency. One more thing they think about is the response of the scintillating materials to temperature and moisture, for example, high purity germanium detector is better than **NaI (TI)** in resolution, but it is sensitive to temperature, where it is supposed to be kept in the vicinity of liquid nitrogen, where a change in temperature is enough to affect HPGE's reactivity and super conductivity that is responsible for its low decay time. On the other hand **NaI (TI)** is very sensitive to moisture, and supposed to be covered with an aluminum layer to protect it.

One more point in our comparison and choice of detectors is the price and recovery expenses of the system, where HPGE for example is very expensive in comparison to NaI (TI), and easily get defected. And in brief words NaI (TI) is recommended for all nuclide identification applications because it provides the best currently available energy resolution for gamma rays in a room temperature. It is a detector that is relatively inexpensive and available in a wide variety of sizes. NuSAFE offers various sizes of NaI(TI) detectors from 2×2" to 4×4×16" arrays depending on your application (NUCSAFE 2016) [45]. NaI(TI) covers a wide range of energy in determination of the peaks, NaI (TI) have a good light yield and excellent linearity (Knoll 2010) [24]. Too many scintillating materials have been invented in the race to satisfy the required conditions or applications. A great table was created by Stephen Derenzo, Martin Boswell, Marvin Weber, and Kathleen Brennan at the Lawrence Berkeley National Laboratory with support from the Department of Home land Security, (USA) (Derenzo, Boswell et al. 2015) [46].

The part in the middle of the 905-3 NaI(TI) Scintillation Detector is the photo multiplier tube (PMT). PMT is a vacuum tube that consists of a photo cathode and several stages of electron multiplying surfaces called dynodes. As soon as the photons of light coming out of the scintillator get translated into electrons through the photocathode, these electrons starts being accelerated towards the successive dynodes, along the PMT, and toward the anode, where the potential difference is build such that these electrons starts to duplicate at their collision with the first dynode as shown in figure 2.9 below. PMT is susceptible to gain instability and non-linearity. A preamplifier is build close to the last dynode, which is the tenth one, to magnify the signal before any noise gain emerges (Hossain, Sharip et al. 2012) [47].

The last part on the right is the fourteen pin connector that connects the 10 dynodes, the cathode, the anode, the focus and the internal line to the high voltage power supply as shown in the figure below:

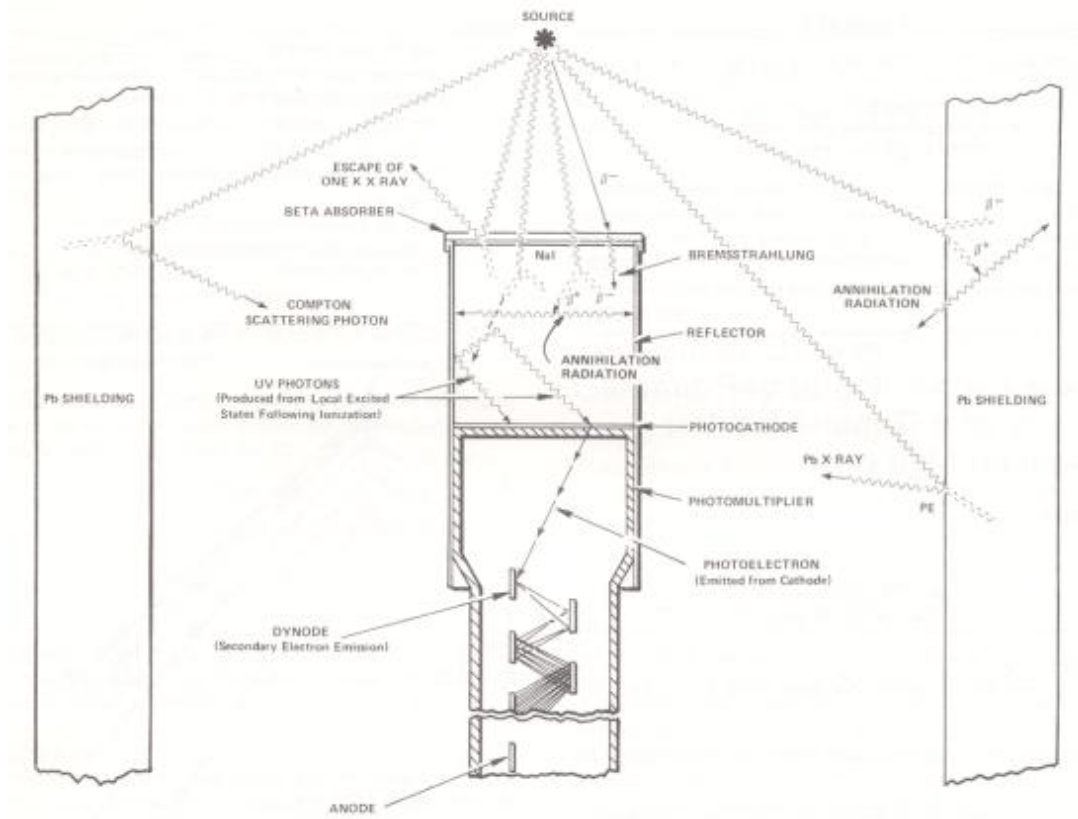


Figure 2.9: A demonstrative drawing for the mechanisms of 905-3 NaI(Tl) (ORTEC) [48].

Next to the 905-3 NaI(Tl) Scintillation Detector, an amplifier is integrated to raise the signal to the proper level that the next part, which is the multichannel analyzer (MCA), requires to be able to read the signal.

2.3.2 Multichannel analyzer

Next part is the Multichannel analyzer (MCA). MCA is a device that sorts signals according to the voltage amplitude of the pulses presented to its input, this signal that is being sorted is the output of the amplifier mentioned above. An MCA is the combination of an analog to digital converter (ADC), a digital histogrammer, and a visual display (Hossain, Sharip et al. 2012) [47]. The ADC converts the height of the input pulse into a digital value, where this value represents the photon energy that was received by the photocathode. After conversion of the signal to digital values the MCA logic gates has the designed property of assigning the distribution of energies received to its available channels linearly, it does have a memory that can save the sorted values and add them up. MCA provides visual display of the resulting distributions, it can also output the data to a printer or computer for further analysis (ORTIC 2010-2014) [5].

As we said above visual display of the MCA could be directed to a computer for sophisticated analysis, scintvision will be doing these analysis. Scintvision 32 could be regarded as an upgrade of maestro 32, it has the properties of graphical user interface for all the controls needed to adjust the acquisition parameters, acquire the data and save the spectra, identifying peaks, editing libraries, and creating it, printing and saving Regions of Interest (ROI)s, performing energy calibrations, automating tasks through job stream. Extra properties with scintvision-32 is isotope identification, activity quantification, peak determination, ScintiVision provide extensive menus and controls for the operation of all acquisition and analysis features, and in brief words with minimum input you get maximum output.

2.3.3 High voltage power supply

The other instrument in our system is a high voltage power supply being used for operating the photo multiplier tube, it ranges in value from 500V to 1100 V, this voltage is supposed to offer the proper potential for the electrons to gain the proper velocity within a short distance to be able to liberate electrons and duplicate itself at each of the anodes.

2.4 Calibration

2.4.1 Energy calibration

Calibration of our spectrum is the assignment of certain known energies to the right channels. To make this calibration we need to do two steps: first one is to get a reference source with elements covering the range of energy our samples is proposed to have, which is supposed to be in the range of 3000 keV, or in other words it is supposed to have enough isolated singlets over the entire range of energy. The (MBSS 2) reference data is shown in table 2.1 below. This reference is inserted in the cavity shown in figure 2.5 above and within a plastic marenilli as if it is a sample, then we start data acquisition. Second step is to make the resulting spectrum build in shape and conform to the reference values of activity peak positions in channel numbers, where this is done through adjustment and choice of the proper voltage and capacitance of the preamplifier. In our system the MCA handles the computer values classified in channels ranging from 0 to 511, for example ^{137}Cs is known to have its peak at channel 280, if we get that and other elements of the reference source, we are then done with the first step of calibration. Next step of

calibration is done by assigning channels to energy values given in the certificate to help scientist build the mathematical relation that helps it find and capture generally any peak, and that could be done any time after acquisition.

Table 2.1: (MBSS 2) Reference Nuclides

Radionuclide	Half-life in days	Activity in Bq	Combined standard uncertainty
Am-241	157800	4214	1.1
Cd-109	462.6	1374	1.5
Ce-139	137.5	0883	1.1
Co-57	271.26	0781	1.1
Co-60	1925.4	2461	1.1
Cs-137	11019	2309	1.2
Sn-113	115.1	3017	2.2
Sr-85	64.78	4843	1.5
Y-88	106.6	4020	1.2
Hg-203	46.72	2218	2.4

In below is shown our reference spectrum acquired

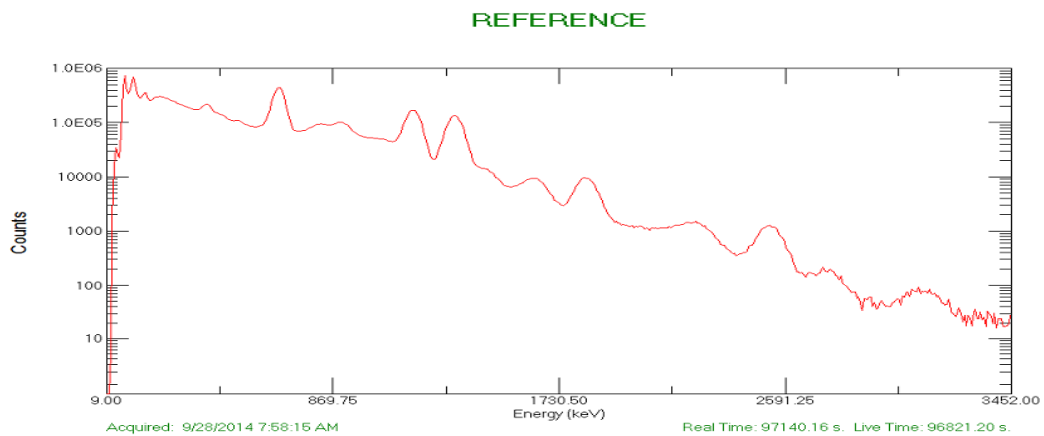


Figure 2.10: Reference spectrum.

After calibration we came up with the governing energy to channel assignation table and curve shown below:

Table 2.2: Resulting energy versus channel number of the used reference nuclides.

Reference nuclide	channel number	Peak energy (K ev)
Ce-139	23	165.85
Sn-113	56.69	391.71
Co-60	196.85	1332.51
Y-88	271.45	1836.01
La-140	375.21	2521.83

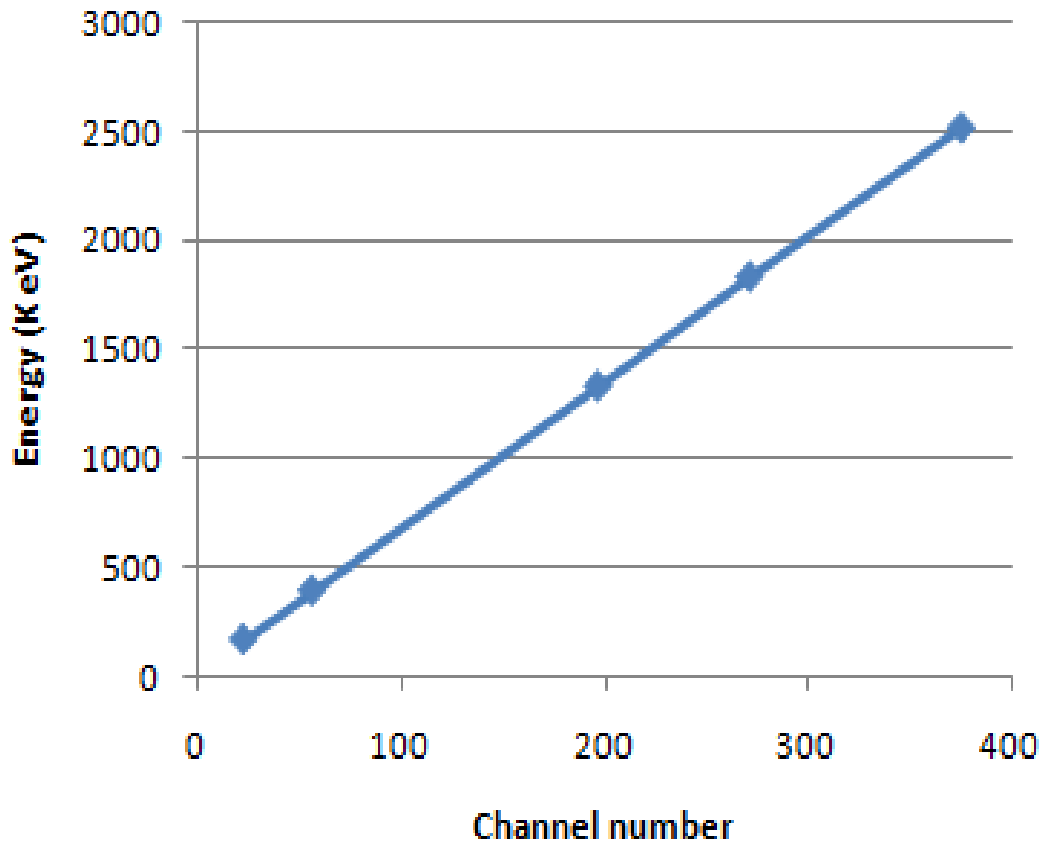


Figure 2.11: Resulting energy versus channel number of the used reference nuclides.

2.4.2 Efficiency calibration

In talking about efficiency, we mean that our instruments don't allow us to achieve our data or measurements that we are supposed to get relative to theoretical and experimental predicted activities listed in published libraries. In our beam line, flux of gamma rays to the scintillator or exposure of the scintillator is dependent on the geometry of the source to scintillator, where this is a matter of study as you can see in the theoretical work of (El-Khatib, Badawi et al. 2013) [49]. On the other hand, not all the gamma ray could interact with scintillator material, where some could penetrate through and leave without being registered, and to predict that you need to study the interaction through the probability wave function of the scintillating material, same approach or principles applies to the photocathode and the dynodes in the (PMT). To understand that let us look at the following quantitative description: In NaI(Tl) the scintillation efficiency is about 13% for ^{137}Cs γ -

ray, which means that the fraction of 661.62 energy of, ^{137}Cs photons that could be converted into photons is about 86 KeV. The energy per emitted photon in NaI (TI) is 4eV, which means that 21,000 photons reach the photocathode. Photocathode has an efficiency of 15%, which means that out of the 21,000 photons of cesium; only 3,200 photons could be gathered and passed to the dynodes to get amplified then detected. Gain through the amplifier dynodes could duplicate one electron to 10^7 electron or more. This signal will be received by MCA. The bunch of amplified electrons will be considered as an identity used to send it to the proper logic gate to be saved in a distinct memory address in MCA as one unit. Then we get the summation of collected units or signals in the spectrum (Hossain, Sharip et al. 2012) [47]. This is the explanation for the loss in activity. To solve for the lost activity or disintegrations, we need to use our reference source again. Scientvision has the property of efficiency calibration, where it can build up efficiency mathematical behavior approximation depending on the resulting spectrum of the reference source of your choice, that we choose to be the one we used in energy calibration and is shown in figure (2.6) above, or in other words it asks you to load the reference spectrum and to fill its date of collection, its date of certificate measurement and activity, and its combined standard uncertainty, Using the following two equation

$$\epsilon_{ij} = \frac{C_{ij}}{A_i I_{ij}} \quad (2.1)$$

You get the mathematical behavior leading to the actual activities.

Where ϵ_{ij} is the absolute photo peak efficiency, C_{ij} is the net count per second of the reference nuclide peak, A_i is the activity of that nuclide as given by the reference certificate, I_{ij} is the absolute intensity of that gamma transition or could be named the peak appearance probability.

This mathematical behavior will be adopted in extraction of our efficiency values in our calculations, where it is applied to each sample spectrum before it become ready for analysis, and is shown below with energy assigned to efficiency under control of this mathematical behavior.

Table 2.3: Resulting efficiencies versus reference energy peaks used.

Reference nuclide	Peak energy (K ev)	Peak efficiency
Ce-139	165.85	0.304881
Sn-113	391.71	0.157061
Co-60	1332.51	0.005329
Y-88	1836.01	0.005066

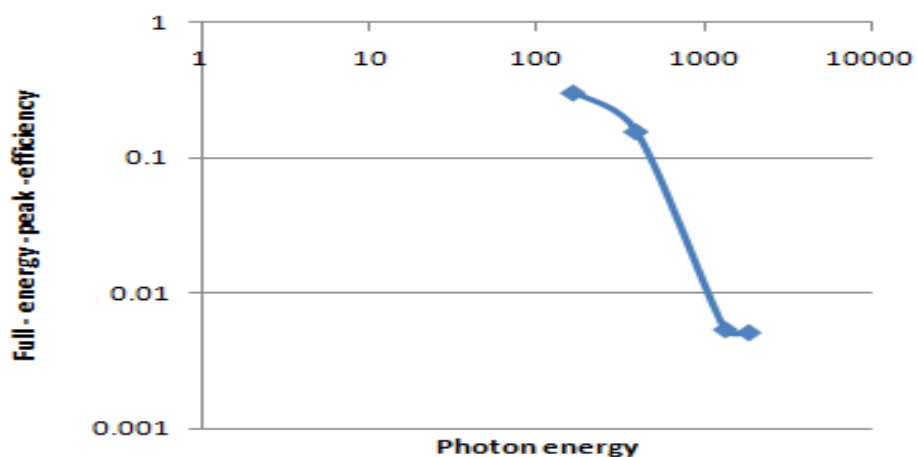


Figure 2.12: Resulting efficiencies versus reference energy peaks used.

In below are shown the tables of probability and efficiencies of each isotope peak of energy diagnosed in our samples:

Table 2.4: U-238 Daughters peaks with their efficiencies and probabilities of appearance shown.

Code	Daughters of U-238	Peak energy(K ev)	peak Efficiency	Peak Probability
a1	BI-214	1238.11	0.0203	0.0592
a2,b4	BI-214	1377.65	0.005304	0.0402
a3	PA-234	230.74	0.2625	0.065
a4	PA-234	692.5	0.1075	0.013
a5,a10	BI-214	1120.28	0.0393	0.1504
a5,a8	PA-234	1394.1	0.005297	0.039
a5	BI-214	1154.77	0.033724	0.0169
a6	PA-234	202.9	0.281166	0.011
a7,a9	PB-214	295.22	0.220201	0.192
a7,b2	PA-234	372.2	0.169839	0.015
a10,c1	PA-234	733	0.101339	0.085
a10	BI-214	934.05	0.068911	0.0316
a10	PA-234	745.35	0.099189	0.03

b1	PA-234	520.6	0.1352	0.012
b2	PA-234	1452.6	0.236509	0.012
b3	BI-214	1729.6	0.005122	0.0305
b4	BI-214	771.86	0.005173	0.0489
c1	PA-234	506.8	0.1372	0.014
c2	PA-234	669.8	0.11116	0.015
c1,c2,c3, c4	PA-234	458.6	0.14494	0.015
c2	RA-226	185.99	0.2855	0.0328
c4	BI-214	665.45	0.050521	0.0156

Table 2.5: Th-232 Daughters peaks with their efficiencies and probabilities of appearance shown.

Code	Th-232 daughters	Peak(K ev)	Peak probability	Peak efficiency
a1,a6	AC-228	328	0.0336	0.1381
a2,a8,b4	AC-228	772.1	0.0162	0.094889
a2,a3,a8,b4	AC-228	911.07	0.29	0.07235
a4	AC-228	129.1	0.0293	0.329
a4,a7,b1	TL-208	763.3	0.017	0.0963
a5	TL-208	277.36	0.065	0.231887
a4,a7,a8,a9,a10,b3	TL-208	2614.47	1	0.00466
b2,c2	AC-228	1587.9	0.0371	0.005818
b3,c1	AC-228	270.3	0.0377	0.236
b3,c1	AC-228	338.4	0.1201	0.192
b4	AC-228	1630.4	0.0195	0.005173
c3	BI-212	1620.56	0.0275	0.00518
c3	PB-212	238.63	0.0431	0.133126
c3	RA-224	241	0.039	0.203737
c4	AC-228	794.8	0.0484	0.036508

Table 2.6: U-235 Daughter (TH-227) peaks with their efficiencies and probabilities of appearance shown.

Code	U-235 daughter isotope	Peak(K ev)	Peak probability	peak Efficiency
a1	TH-227	256.25	0.068	0.188
a5	TH-227	286.15	0.0158	0.164
a6	TH-227	299.9	0.02	0.155
a6	TH-227	304.35	0.0105	0.152
b3	TH-227	329.82	0.0275	0.138

Table 2.7: K-40 isotope peak probability and efficiency.

Code	Isotope	Isotope probability	Isotope efficiency
All samples	K-40	0.107	0.007746155

Table 2.8: Cs-137 isotope peak probability and efficiency.

Code	Isotope	Isotope probability	Isotope efficiency
All samples	Cs-137	0.8462	0.050893

Table 2.9: J-135 peaks with their efficiencies and probabilities of appearance shown.

Code	Isotope	Peak(K ev)	Peak probability	Peak efficiency
a2,a4	J-135	1678.03	0.0952	0.00471
a3	J-135	220.5	0.0175	0.226
a3,b1	J-135	526.56	0.1333	0.0734
a3,c2	J-135	1457.56	0.0864	0.00784
a4,b3,b4	J-135	1706.46	0.0409	0.00445
a5	J-135	1124	0.036	0.01665
a5	J-135	288.45	0.0309	0.162
a7	J-135	546.56	0.0712	0.0694
b3,b4	J-135	1791.2	0.0769	0.0037
b3	J-135	1131.51	0.2251	0.01642
c1	J-135	417.63	0.0352	0.1014

Table 2.10: Contamination nuclides with their peaks probabilities and efficiencies shown.

Code	Isotope	peak (K ev)	Peak probability	Peak efficiency
a5	BA-140	423.69	0.0266	0.150863
b1,c2	BA-140	437.55	0.0155	0.148707
c2	BA-140	162.64	0.0507	0.307
c2	BA-140	304.82	0.0365	0.214
a7,a9	MO-99	366.44	0.0121	0.172846
a8,a9	MO-99	739.47	0.13	0.100264
b3,c3,c4,b2	SB-125	380.51	0.014	0.16401
a9,a10	SB-125	428.09	0.296	0.149785
a6,a10	CS-134	1365.13	0.0304	0.005312
a9	CS-134	1167.86	0.018	0.031581
b3	CS-134	475.35	0.0146	0.142241
c4	CS-134	795.76	0.854	0.091
a7	NB-95	765.82	0.99	0.095964
a1,a3	J-131	364.48	0.8124	0.175
a5	J-131	284.29	0.0606	0.2275

2.5 Measurement of background

Background radiation is due to any radiating material that could exist in the system material or its peripherals other than the sample being measured.

To measure the background spectrum we are supposed to turn on our system with plastic marenilli inserted in the measurement cavity for the same period of time that will be applied to each sample. This background spectrum will be saved for analysis, where it will be subtracted from each of the sample spectrums. Background was measured after the preliminary calibration was done to the system, and the resulting spectrum shown in Figure 2.13.

After second step of calibration is done, it was applied to the background to be ready for its analyses, its analysis results was then edited and saved as peak background correction library (PPC) that you will be asked to submit it to sample analysis preset values in the analysis menu bar in preparing for sample analysis.

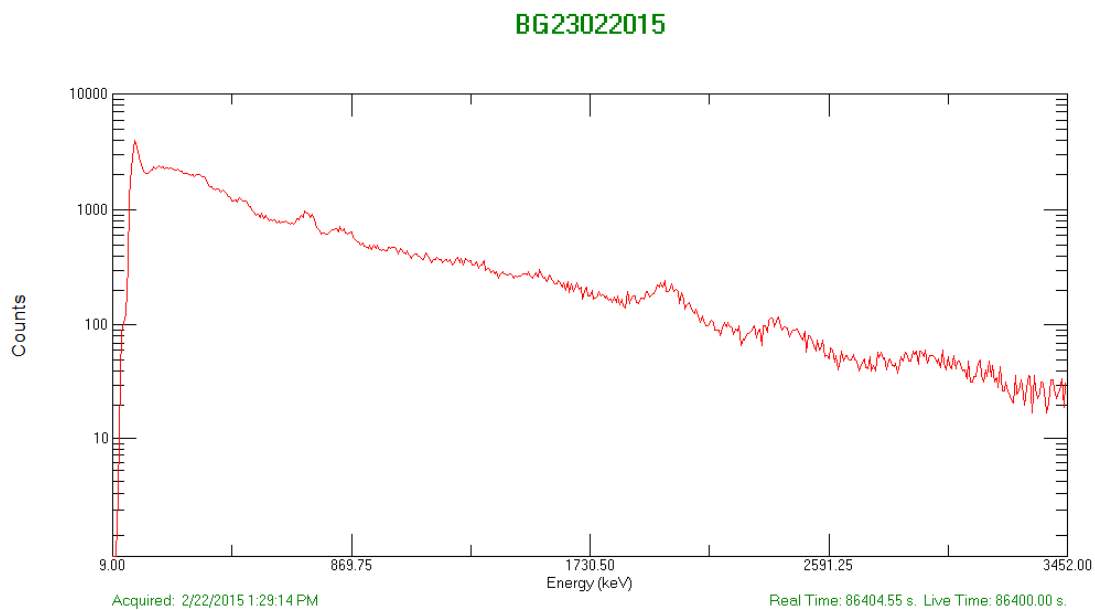


Figure 2.3: Resulting background spectrum.

2.6 Sample measurement and analysis

Each of our samples was inserted in the calibrated system for 24 hours to get the best possible acquisition, as soon as it is known that we are dealing with weak radiating

sources, or samples. These spectrums had been acquired and saved to computer disk in scintvision file format SPC, and ready for analysis, one of these spectra is shown below:

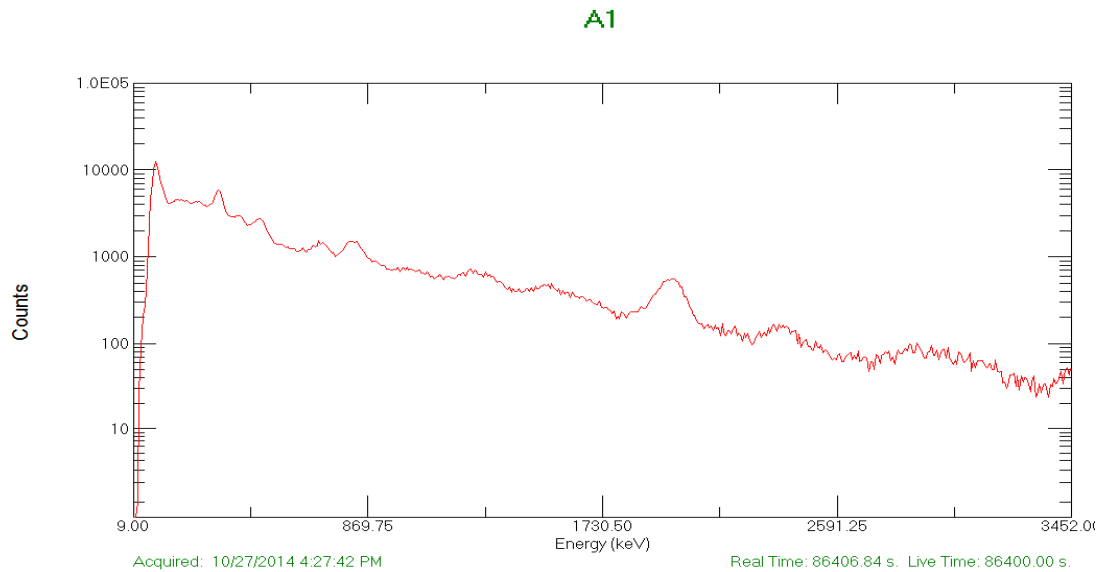


Figure 2.14: Resulting spectrum for sample one as a typical form.

Our analysis starts by second step of energy calibration we talked about earlier, which is the assigning of the peaks energies to channels under energy calibration within toolbar to let scientvision build its mathematical code, according to reference certificate, just like peaks was assigned to channels when calibration prior to acquisition was done. In building up such calibration we depend on our reference that was put under acquisition and its spectrum was saved to disk beside our samples, we were supposed to start that with the most famous peaks like ^{137}Cs and ^{60}Co , to use them as a stabilizer to calibration, in each of these peaks, starting by the famous and sharp ones and choosing of them far apart, we started by marking regions of interest, then assigning the reference given values, entering these values up to last one. Next to that will be the efficiency calibration of the reference measured spectrum. This resultant energy efficiency calibration is supposed to be applied to the spectrums one by one before it gets ready for analysis.

Fulfilling requirements of data analysis, we applied the command of data analysis for the sample spectrums one by one, with that we get reports of the elements found in the samples, which includes: peak channel, centroid energy, background counts, net area counts, intensity, uncertainty, and full width at half maximum (FWHM).

Chapter Three

Theoretical calculations in relation to activity

Chapter Three

Theoretical calculations in relation to activity

3.1 Introductory to activity concentrations calculation

Our study comes in the level of studying the NORM activities depending on approximately pure soil samples. Mainly ^{238}U , ^{235}U , ^{232}Th , and ^{40}K , have been found. On the other hand we need to get an estimation of the artificial radiating materials activity concentrations that is supposed to appear in our samples.

A plenty of peaks were found out in our spectrum analysis. As it is supposed to happen, none of the two main radioactive series ^{238}U and ^{232}Th nuclides was found, but their daughter nuclides did, table (2.1) below shows the peaks found and used to calculate the activity concentrations of ^{238}U , ^{232}Th and ^{235}U claiming secular equilibrium. Calculation is performed using the famous equation used by (Erees, Akozcan et al. 2006) [50]:

$$A_i = \frac{C_{ij}}{I_{ij}\epsilon_{ij}M_S} \quad (3.1)$$

Where C_{ij} stands for counts rate, I_{ij} stands for nuclide i peak j probability, ϵ_{ij} stands for peak efficiency, and M_S stands for samples weight.

Next will be the calculation of ^{40}K as an appreciable NORM nuclide, with its peak at 1460 keV, and considered the last term required toward the calculation or estimation of radium equivalent activity and other dependent quantities. Another important friend for ^{40}K is ^{137}Cs with its famous peak at 661.62 KeV, which will be included in NORM nuclides processing.

For ^{235}U , the parent nuclide was found through its peaks that are below 125 KeV, where the efficiency curve does not support that range of energy, but among its daughter nuclides, ^{227}Th was determined, and so the concentration activity will not be calculated directly using ^{235}U peaks, but in scope of secular equilibrium with its daughter ^{227}Th .

Table 3.1: Diagnosed peaks of each of U-238, Th-232 and U-235 daughter nuclides.

²³⁸ U daughter nuclides		²³² Th daughter nuclides		²³⁵ U daughter nuclides	
Nuclide	peak(K ev)	nuclide	Peak(K ev)	nuclide	peak(K ev)
Pa-234	202.9	Ac-228	129.1	Th-227	256.25
Pa-234	230.74	Ac-228	270.3	Th-227	286.15
Pa-234	372.2	Ac-228	338.4	Th-227	304.44
Pa-234	458.6	Ac-228	772.1	Th-227	329.82
Pa-234	506.8	Ac-228	794.8	Th-227	299.9
Pa-234	520.6	Ac-228	911.07		
Pa-234	669.8	Ac-228	916.03		
Pa-234	692.5	Ac-228	1587.9		
Pa-234	733	Ac-228	1630.4		
Pa-234	745.35	Bi-212	1620.56		
Pa-234	1353	Tl-208	277.36		
Pa-234	1394.1	Tl-208	763.3		
Pa-234	1452.6	Tl-208	2614.47		
Ra-226	185.99	Pb-212	238.63		
Pb-214	295.22	Ra-224	241		
Bi-214	771.86				
Bi-214	934.05				
Bi-214	1120.28				
Bi-214	1154.77				
Bi-214	1238.11				
Bi-214	1377.65				
Bi-214	1729.6				

3.2 Calculation of dose rates and indices.

3.2.1 Radium equivalent activity

This value is a representative to the NORM radiation effects, and is related to ²³⁸U, ²³²Th, and ⁴⁰K activity concentrations through the following relation used by (Huy and Luyen 2006, Dabayneh, Mashal et al. 2008) [34, 51]:

$$Ra_{eq}(BqKg^{-1}) = A_u + 1.43 \times A_{Th} + 0.077 \times A_k \quad (3.2)$$

Where A_u , A_{Th} and A_k are the activity concentrations of ²³⁸U, ²³²Th, and ⁴⁰K respectively.

3.2.2 Absorbed dose rate in air

Radioactivity concentrations of NORM nuclides ²³⁸U, ²³²Th, and ⁴⁰K are related to exposure according to the following mathematical relation used by (Dabayneh, Mashal et al. 2008) [34]:

$$D_r \left(\frac{nGy}{h} \right) = 0.427 \times A_u + 0.662 \times A_{Th} + 0.043 \times A_k \quad (3.3)$$

where $D_r \left(\frac{nGy}{h} \right)$ is the absorbed dose rate considered at 1 meter above earth surface concerning air molecules, an equivalency to hazard effect values in relation to human will be discussed.

Calculation for ^{137}Cs concentration activity as an artificial contamination radionuclide was done, and was included in the outdoor air absorbed dose rates. Equation 3.3 was modified to include not only the ^{137}Cs term but also the cosmic radiation effect (Dabayneh, Mashal et al. 2008) [34]:

$$D_r \left(\frac{nGy}{h} \right) = 0.427 \times Au + 0.662 \times A_{Th} + 0.03A_{Cs} + 34 \quad (3.4)$$

where A_{Cs} is the concentration activity of ^{137}Cs , and the number 34 is a factor included to ensure that the effects of the cosmic rays are implemented.

3.2.3 Annual effective dose equivalent

This value is introduced to estimate the effect of the absorbed dose on human health, this effect was found to be dependent on age as we discussed earlier, the idea was translated into mathematical coefficients, the UNSCEAR 2000 report depended avalue of 0.8 Sv/Gy for children, 0.9 Sv/Gy for infants and 0.7 Sv/Gy for adults, where the last value will be used in calculation as a representative value. One more coefficient is the indoor of 0.8 and outdoor of 0.2 depending on percent of time a person spend in and out, these values are estimated annually, which means a period of one year. a coefficient of 1.4 is used in the $D_{indoor}(mSvy^{-1})$, where that resulting increment is due the walls considered as sources on one hand and as a reflector on the other hand as was shown in talking about gamma ray interaction with mater. The mathematical expression used to calculate these values as used by (ABU SAMREH, THABAYNEH et al. 2014) [39] is:

$$D_{outdoor}(mSvy^{-1}) = D_r(mGyh^{-1}) * 365.25 * 24h * 0.2 * 0.7SvGy^{-1} * 10^{-6} \quad (3.5)$$

$$D_{indoor}(mSvy^{-1}) = D_r(mGyh^{-1}) * 365.25 * 24h * 0.8 * 0.7SvGy^{-1} * 10^{-6} \quad (3.6)$$

$$D_{total}(mSvy^{-1}) = D_{outdoor} + D_{indoor} \quad (3.7)$$

3.2.4 External hazard index

It is, as the name says, an index came as a result of Ra_{eq} divided by 370 (Bq/Kg), which was estimated as an upper value for Ra_{eq} . That means the index should be below one to be in the safe threshold. The mathematical form as used in (Huy and Luyen 2006, Dabayneh, Mashal et al. 2008) [34, 51] is:

$$H_{ex} = \left(\frac{A_U}{\frac{370 \text{ Bq}}{\text{kg}}} + \frac{A_{Th}}{\frac{259 \text{ Bq}}{\text{kg}}} + \frac{A_K}{\frac{4810 \text{ Bq}}{\text{kg}}} \right) \leq 1 \quad (3.8)$$

3.2.5 Internal hazard index

It is an estimation of hazard level of alpha radiation emitted by radon gas that originates from the ^{238}U and ^{232}Th decay chains, and it has the following mathematical form used in (Dabayneh, Mashal et al. 2008, ABU SAMREH, THABAYNEH et al. 2014) [34, 39]:

$$H_{in} = \left(\frac{A_U}{\frac{185 \text{ Bq}}{\text{kg}}} + \frac{A_{Th}}{\frac{259 \text{ Bq}}{\text{kg}}} + \frac{A_K}{\frac{4810 \text{ Bq}}{\text{kg}}} \right) \leq 1 \quad (3.9)$$

3.2.6 Radioactivity level index

It is an index representing the safe level of the outdoor air- absorbed dose rate relative to a proposed value of 64 nGy/h, where this value has to be less than or equal to one, and represented the following way as used in (Huy and Luyen 2006) [51]:

$$I_\gamma = \frac{A_U}{150 \text{ BqKg}^{-1}} + \frac{A_{Th}}{100 \text{ BqKg}^{-1}} + \frac{A_K}{1500 \text{ BqKg}^{-1}} \leq 1 \quad (3.10)$$

This index value is calculated and will be shown in results.

3.3 Details about contamination products

Beside ^{137}Cs there was a punch of nuclides that are related to fission product yield, we calculated their activities and, also J_{135} as a contamination element, which is being used, and produced in large amounts as fission product in nuclear planet, it is a controller in itself, it is a weak neutron absorber, and in its decay product Xe_{135} is a strong absorber and regarded as reactor poison. To achieve the proper power rate for the reactor, there should be a permanent disposal of J_{135} and Xe_{135} . Disposal of such amounts could be claimed as the reason behind the activities we found

for J_{135} in most of our samples, and its short half life could be good evidence that its source is close enough to the area of study. J_{135} as a fission product in nuclear tests is considered as a vanishing element depending on its short half life in comparison to the flight time the airborne effluent products or yields takes to spread and reach the inhabited areas, but if we consider its huge amount as a fission product, it could reach and land to ground and get detected, so we can consider it as a factor within our measured activity.

Table 3.2: J-135 diagnosed peaks with the sample codes that each peak was found in.

Code	J_{135} peaks (K ev)
b3, b4	1791.2
a4, b3, b4	1706.46
a2, a4	1678.03
a3, c2	1457.56
a5	1124
b3	1131.51
a7	546.56
a3, b1	526.56
c1	417.63
a5	288.45
a3	220.5

Concerning other than J_{135} contamination nuclides, a table below is showing the nuclides peaks found listed, where activity concentrations will be calculated, a list of these nuclides found in our samples are listed below in table 3.3.

Table 3.3: Fission product yeild nuclides peaks diagnosed with codes of the samples they were found in.

Code	Nuclide	Peak (K ev)
a5	Ba-140	427.2
b1, c2	Ba-140	437.55
c2	Ba-140	164.74
c2	Ba-140	304.82
a7, a9	Mo-99	366.44
a8, a9	Mo-99	739.47
b3, c3, c4, b2	Sb-125	380.51
a9, a10	Sb-125	428.09
a6, a10	Cs-134	1365.13
a9	Cs-134	1164.03
b3	Cs-134	475.35
c4	Cs-134	795.76
a7	Nb-95	770.58
a1, a3	J-131	364.48
a5	J-131	284.29

Chapter Four
Results, Reasoning, Comparasions, and Conclusions

Chapter Four

Results, Reasoning, Comparasions, and Conclusions

4.1 introduction

The 2" x 2" NaI(Tl) Detector was used as the core part toward acheiving our results of determination of radioactive contents and calculation of their activity concentrations and the related radiological parameters and indeses. In the following pages we will be showing the NORM concentration levels values in average form with the ranges of values in a table, ^{137}Cs will be shown in the same table, following previous studies in where they used to consider it as a family member of the norm nuclides, that will be a companied with worldwide averages according to (UNSCEAR 2000) report [13]. Next to that will be a brief table showing the overall averages of the radiological parameters and indices. A table of ^{235}U will be shown followed by some remarks. J_{135} concentration activities is demonstrated too. Atable of nuclear fission yeild nuclides concentration activities with column chart is shown in comparasion with JWB at English Wikipedia column chart of fission product yeild.

4.2 Results of NORM

4.2.1 Results and comparasions of U-238, Th-232, K-40, and Cs-137

Detailed calculated values for ^{238}U , ^{232}Th , ^{40}K and ^{137}Cs in our collectd samples is shown in table B1 in appendix B, and the addresses of collection are shown in table A1 in appendix A. In table 4.1 below, the overall average of the samples is shown compared to world wide average given by (UNSCEAR 2000) report[13], same is the case with the values range.

Table 4.1: Activity concentration of NORM nuclides and Cs-137 compared to national values.

Nuclide	Our study average	Worldwide average	Our study range	World wide range
$A_{U_{238}}$	57.0 ± 9.7	35	5-168	16-110; [13]
$A_{Th_{232}}$	47.9 ± 6.0	30	2-98	11-64; [13]
$A_{K_{40}}$	78.0 ± 8.9	400	35-127	140-850; [13]
$A_{Cs_{137}}$	1.2 ± 0.1	----	0.16-2.45	-----

The results of analysis of activity concentrations of ^{238}U , ^{232}Th , ^{40}K and ^{137}Cs radionuclides in all samples of the different locations of the study area are presented in table 4.1.

The range of measured activity of ^{238}U in all samples in the area under investigation was 5 to 168 Bq Kg^{-1} with an average value of 57 Bq Kg^{-1} . The differences in values are attributable to geochemical composition and origin of soil types in a particular area. The range of measured activity concentrations of ^{232}Th for the samples was 2 to 98 Bq Kg^{-1} with an average of 47.9 Bq Kg^{-1} . The activity concentrations of ^{40}K was 35 to 127 Bq Kg^{-1} with an average value of 78 Bq Kg^{-1} . The observed results in some samples show that the activity concentrations for ^{238}U , and ^{232}Th for the investigated sites are higher than the reported international radioactivity levels of ^{238}U , and ^{232}Th in UNSCEAR 2000 report. The recorded high values of the radionuclides in some of the samples may be due to the presence of radioactive-rich granite, phosphate, sandstone, and quartz.

The radionuclide ^{137}Cs was detected in all of the locations, which is likely due to fallout of previous worldwide nuclear explosions and reactor accidents.

Comparison information for ^{137}Cs were adopted from (Dabayneh, Mashal et al. 2008) [34], beside that (Rafique 2014) [52] got an average for activity concentration for ^{137}Cs of $(1.39 \pm 0.17) \text{BqKg}^{-1}$, and his values ranging from 0.33 to 2.93BqKg^{-1} , where his result seems to be consistent with ours. In relation to NORM nuclides, our results seem to be different from worldwide values, but it is within its range of values. Values for A_K seems to be low relative to worldwide average, and that could be due to high solubility of potassium in rain water, where our samples didn't contain rocks, this could be understood through this abbreviation "granite is a common rock and potassium is abundant there". K-40 is incompatible in basalt as well and leaves it as soon as possible (when basalt melts). And so it goes until very evolved rocks like granite form that contain significant amounts of potassium that is gathered from tens of times larger volumes of molten peridotite (Sandatlas) [53], what we can get out of this abbreviation is that our values average could be a lot less than rocky samples and so the world wide range of values.

4.2.2 Results of dose parameters and indices

Below is a table showing the results of $Ra_{eq}(Bq/Kg)$, $D_r(nGy/h)$, $D_\gamma(nGy/h)$, $D_{outdoor}(mSvy^{-1})$, $D_{indoor}(mSvy^{-1})$, $D_{total}(mSvy^{-1})$, H_{ex} , H_{in} , and I_γ averaged over samples.

Table 4.2: Radiation dose parameters average values compared to worldwide values.

Parameter symbol	Our study values	Worldwide values
$Ra_{eq}(Bq/Kg)$	131.5±15.1	-----
$D_r(nGy/h)$	59.4±6.7	51.0; [13]
$D_\gamma(nGy/h)$	93.4±6.7	-----
$D_{outdoor}(mSvy^{-1})$	0.0729±0.0057	0.07; [13]
$D_{indoor}(mSvy^{-1})$	0.4081±0.0057	0.41; [13]
$D_{total}(mSvy^{-1})$	0.481±0.0114	0.48
H_{ex}	0.3551±0.0407	-----
H_{in}	0.5092±0.0663	-----
I_γ	0.9108±0.0150	-----

Our values above are close enough to worldwide average values, and within the safe to health limits.

4.2.3 U-235 activity concentration

^{235}U as a NORM nuclide is calculated and shown in table 4.3 below:

Table 4.3: Results of U-235 activity concentrations in average form through its daughter nuclide Th-227.

Range of Th-227 values	(0.376-5.819) $BqKg^{-1}$
Average of Th-227 Activity concentration	(3.151±0.326) $BqKg^{-1}$

As can be seen, calculation of ^{235}U activity concentration through secular equilibrium with its daughter ^{227}Th . (Harb, El-Kamel et al. 2008) [54] shows an average of (2.23±0.21) $BqKg^{-1}$, and values range of (1.16±0.11 to 4.83±0.44) $BqKg^{-1}$ for ^{235}U activity concentration, where that seems to be close enough to our values.

4.3 Results and comparasions of contamination elements

4.3.1 J-135

In talking about contamination elements, we found J_{135} in most of our samples, this element is a fission product yield entity. The average concentration activity over peaks and samples is $(66.596 \pm 8.524) BqKg^{-1}$, and its range is $(1.5-158) BqKg^{-1}$ as can be seen in table C1 in appendix C. For this study as can be seen in table C1 averages for a and b samples seems to be the same, samples c does not give dependable increment in average until we get more samples from that destination in our coming study. A hypothetical accident study was done by (Malek, Chisty et al. 2012) [55] to estimate iodine fission products isotopes activity concentrations through different geometrical directions and through its ingestion and penetration to living things. Their estimation was done at 110 meter a round TRIGA Mark-II research Reactor at AERE, Savar, Bangladesh. They got an average over value and direction for J_{135} ground concentration of $(83454 Bqm^{-2})$, by no mean this is similar to our values, but if they take their measurements 10^5 meter in place of 110 meter away from the reactor and without any accident in the nuclear reactor as assumed, in this case I think they will get values similar to ours. The point here is that not only nuclear tests in the air or underground can spread J_{135} , but also nuclear power plants could do that also. The good judge in this argument is a future study determining the rate or change in activity with time and destinations a round hypothetical nuclear power plates and in connection with winds distribution.

4.3.2 Other fission yeild elements

Fission yield elements build up as a result of artificial nuclear activities that includes using of nuclear weapons, accidents in nuclear planets, generation of electricity in nuclear power plants and last is the greatest factor, at least for now on, is the nuclear explosions tests that had been being done in the atmosphere since late forties until about five decades ago when countries started to do their tests underground, and that caused a fall down in contamination concentration activities, where a peak in that was attained in the sixties. In our samples these elements were found and their nuclides activities are shown in appendix C table C2, the average activity over elements is $(52.843 \pm 11.16) BqKg^{-1}$ and its range is $(1.2-134.8) BqKg^{-1}$. Figure 4.1 below is a chart showing activity versus contamination nuclide without J_{135} and Cs_{137} included.

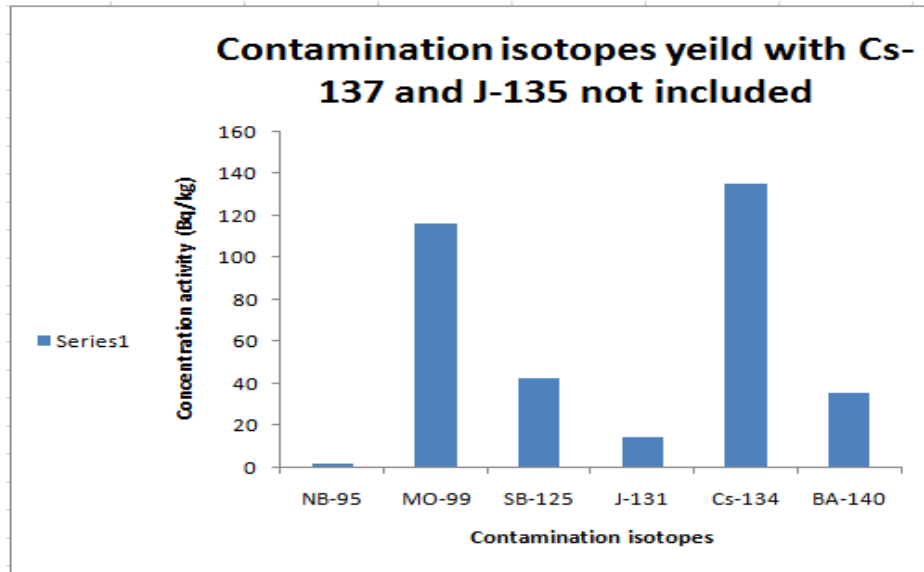


Figure 4.1: Contamination isotopes found in our samples without including J-135 and Cs-137 versus concentration activity chart.

In figure 4.2 below the fision product yeild is shown versus time and element. It could be noticed that our contamination elements approximately behaves like its matches in figure 4.2.

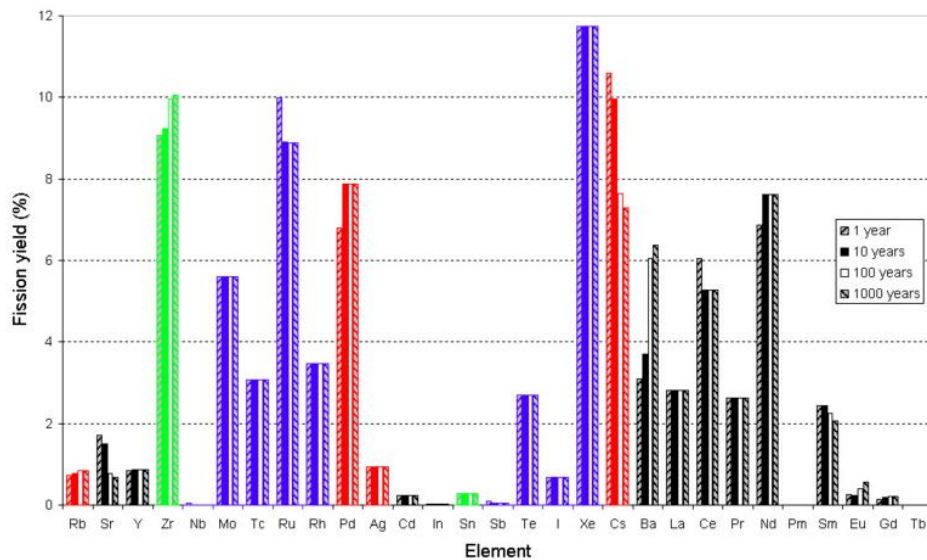


Figure 4.2: Yield of different elements from nuclear fission after different cooling times. This is only a rough estimate. The author did not specify the parent nuclide.

In figure 4.3: below J_{135} and Cs_{137} are included. We can notice that change in Cs due to Cs_{137} is slight, while that of J_{135} is significant, and deforms the consistency with figure

4.2 in J where it could be said that J_{135} concentration activity relates to local nuclear power plants.

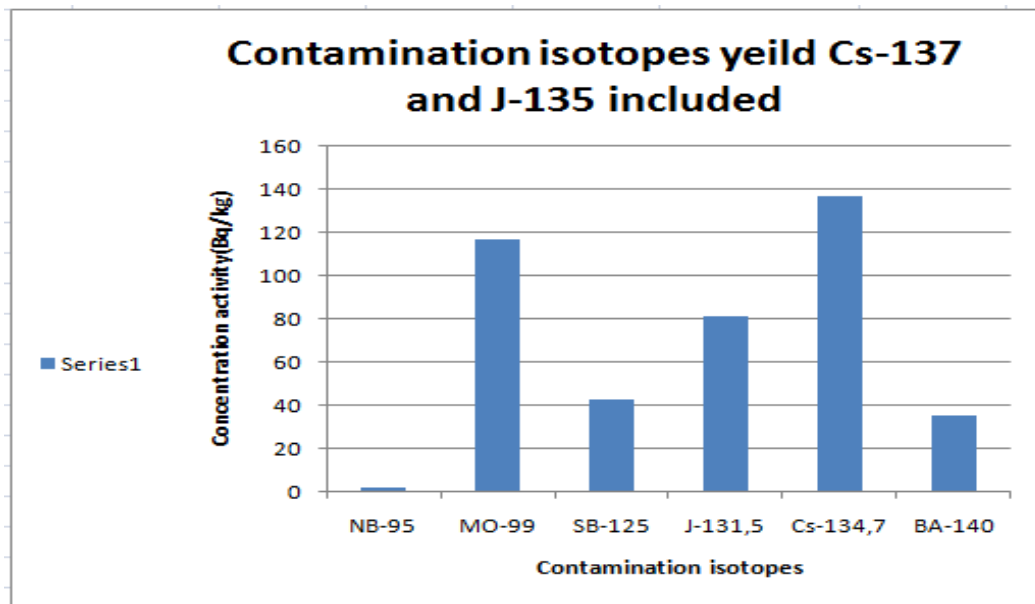


Figure 4.3: Contamination isotopes found in our samples including J-135 and Cs-137 versus concentration activity chart.

The authors in (Trinh Van, Nguyen Quang et al. 2013) [56] talks a bout Fukushima nuclear accident and its airborne deposits in Vietnam from north to south, fifteen days after the accident. The common finding with this study is that mainly among Cs isotopes they found Cs-134, and Cs-137 and among J isotopes they found J-131. Their results appear to support ours.

Chapter Five

Conclusions and Future work

Chapter Five

Conclusions and Future work

5.1 Introduction

Our result of natural and artificial radionuclides average concentration activities in our samples, that were collected over south Bethlehem up till south Hebron in three successive lines going east to west, was shown and discussed in previous chapter, and in brief form, the average concentration activity for the NORM nuclides (^{238}U , ^{232}Th , ^{235}U and ^{40}K) was found to be successively $(57.0\pm 9.7, 47.9\pm 6.0, 3.151\pm 0.326$ and $78.0\pm 8.9) \text{ BqKg}^{-1}$, respectively. ^{137}Cs average concentration activity was found to be $(1.2\pm 0.1) \text{ BqKg}^{-1}$. For contamination product J_{135} , its average concentration activity was found to be $(66.596\pm 8.524) \text{ BqKg}^{-1}$. For other contamination elements, the average concentration activities are shown in appendix C, table C2.

Discussion of these values and the related parameters were done in details in chapter four, where there was no abrupt differences in values relative to local and worldwide results. On the contrary it seems to be mostly descriptive, it goes in accordance with the results of Dabayneh, Mashal et al. 2008) [34] cooperatively with (ABU SAMREH, THABAYNEH et al. 2014) [39] in the values for ^{238}U and ^{232}Th .

5.2 Future work

Depending on our current study, it seems that we need to have more analytical values in relation to contamination products explaining the two major variables that are explanatory to the origin of the deposits we found, these two variables are the amount of deposits and time, in other words you have to collect samples along the time and destinations. Choice of periods of time and places of collection is a matter of introductory study. The rates of changes in activity in this future study can build up an idea about the sources and behaviour of the deposition.

One more aspect in the study in relation to values we got for potassium is to collect rocky samples, soil samples from river banks and bottom of valleys.

It is a motivating aspect and supposed to be considered a duty is the studies in medical physics concerning the defects due to radiation caused to living things, and the more important is to devote radiation in cure of diseases including cancer under radiation therapy.

One important note, need to be said, is that even though I have to defend 905-3 NaI(Tl), as my system of measurement, and the scientists behind this system, It seems to me that I should explore the properties of HPGGe detector in my future work.

Appendix A

Table A :The list of sample's site of collection addresses.

Code	Adress
a_1	Wad alhuroob – Assamu' – South Hebron
a_2	Ammenwaar – Assamu' – South Hebron
a_3	Assamu'west entrance – Assamu' – South Hebron
a_4	Rabood – Addaheriya – South Hebron
a_5	Kurza – Addaheriya – South Hebron
a_6	Salet Mayar – Wadelkaleel – Addaheriya – South Hebron
a_7	Wad annayjar – Wad alkaleel – Addaheriya – south Hebron
a_8	Mahatat almansiya lelzoyoot – Wad alkaleel – Addaheriya – South Hebron
a_9	Masjed annabi ayoob – Wad alkaleel – Addaheriya – South Hebron
a_{10}	Montazah abu karoob – Arramadeen – Addaheriya – South Hebron
b_1	Ayn Sa'eer – Sa'eer – South Hebron
b_2	BeitUmmar – North Hebron
b_3	Annabiyounes – Hulhol – North Hebron
b_4	Bakkar – Halhl – North Hebron
c_1	Tuqu' – South Bethlehem
c_2	Almanshiya – South Bethlehem
c_3	Umm Salamuna – South Bethlehem
c_4	Efrat – South Bethlehem

Appendix B

Table B1: Concentration activities of NORM nuclides and ^{137}Cs .

Code	Activity Concentrations (Bq.Kg^{-1})			
	^{137}Cs	^{40}K	^{232}Th	^{238}U
a1	0.7±0.1	35.6±4.0	98.3±6.6	33.3±2.9
a2	1.0±0.1	127.3±14.5	16.5±1.2	168.8±16.6
a3	0.5±0.1	110.0±12.5	11.2±0.9	4.6±1.1
a4	0.7±0.1	110.0±12.5	21.6±1.8	8.6±2.5
a5	1.8±0.2	51.2±5.8	30.5±2.5	61.9±8.9
a6	1.0±0.1	65.0±7.4	75.6±2.1	79.5±26.1
a7	2.5±0.3	63.3±7.2	70.1±14.4	55.7±1.5
a8	0.5±0.1	97.9±11.1	10.4±0.9	27.2±8.4
a9	2.4±0.3	80.6±9.2	2.1±0.0	15.4±1.3
a10	1.5±0.2	71.9±8.2	3.9±0.5	15.6±2.9
b1	0.3±0.0	37.3±4.2	17.1±2.6	46.6±5.4
b2	2.0±0.2	99.6±11.3	129.7±30.0	47.4±8.6
b3	1.5±0.2	103.1±11.7	24.1±5.8	65.3±8.3
b4	0.2±0.0	56.4±6.4	36.3±7.4	39.2±17.9
c1	1.0±0.1	63.3±7.2	50.2±3.9	97.8±13.3
c2	2.1±0.2	103.1±11.7	92.7±12.2	85.8±17.0
c3	1.6±0.2	73.7±8.4	28.7±5.5	86.5±17.9
c4	1.2±0.1	54.6±6.2	142.6±8.7	87.2±13.1
Average	1.2±0.1	78.0±8.9	47.9±6.0	57.0±9.7

Table B2: Results Radium equivalent activities (Ra_{eq}), outdoor air absorbed dose (D_r), and D_γ for NORM nuclides only.

Code	$Ra_{eq}(\text{BqKg}^{-1})$	$D_r(\text{nGy/h})$	$D_\gamma(\text{nGy/h})$
a1	176.6±12.4	80.8±5.6	114.8±5.6
a2	202.3±16.7	88.5±7.2	122.6±7.2
a3	29.1±1.9	14.1±0.9	48.1±0.9
a4	48.0±3.7	22.7±1.7	56.7±1.7
a5	109.4±9.6	48.8±4.2	82.9±4.2
a6	192.6±26.3	86.8±11.2	120.8±11.2
a7	160.7±20.7	72.9±9.6	107.0±9.6
a8	49.6±8.5	22.7±3.7	56.7±3.7
a9	24.7±1.4	11.5±0.7	45.5±0.7
a10	26.6±3.1	12.3±1.3	46.3±1.3
b1	73.9±6.6	32.8±2.9	66.8±2.9
b2	240.5±46.7	110.4±21.3	144.4±21.3
b3	107.7±16.1	48.3±7.0	82.3±7.0
b4	95.5±20.8	43.2±9.1	77.2±9.1
c1	174.5±14.4	77.7±6.3	111.7±6.3
c2	226.2±24.4	102.4±10.9	136.5±10.9
c3	133.2±19.6	59.1±8.5	93.1±8.5
c4	295.3±18.0	134.0±8.0	168.0±8.0
Average	131.5±15.1	59.4±6.7	93.4±6.7

Table B3: Results of annual effective doses outdoor and indoor.

Code	$D_{outdoor}(mSvy^{-1})$	$D_{indoor}(mSvy^{-1})$	$D_{total}(mSvy^{-1})$
a1	0.0992±0.0051	0.5553±0.0051	0.6545±0.0072
a2	0.1086±0.0064	0.6084±0.0064	0.7170±0.0090
a3	0.0173±0.0033	0.0971±0.0033	0.1144±0.0047
a4	0.0279±0.0008	0.1561±0.0008	0.1839±0.0012
a5	0.0599±0.0030	0.3355±0.0030	0.3954±0.0043
a6	0.1065±0.0099	0.5964±0.0099	0.7029±0.0140
a7	0.0894±0.0080	0.5009±0.0080	0.5903±0.0113
a8	0.0279±0.0018	0.1562±0.0018	0.1840±0.0025
a9	0.0141±0.0002	0.0788±0.0002	0.0929±0.0003
a10	0.0151±0.0005	0.0846±0.0005	0.0997±0.0007
b1	0.0403±0.0019	0.2255±0.0019	0.2658±0.0027
b2	0.1355±0.0204	0.7586±0.0204	0.8941±0.0289
b3	0.0592±0.0045	0.3317±0.0045	0.3909±0.0064
b4	0.0530±0.0074	0.2969±0.0074	0.3499±0.0105
c1	0.0954±0.0052	0.5341±0.0052	0.6295±0.0074
c2	0.1257±0.0100	0.7037±0.0100	0.8293±0.0142
c3	0.0725±0.0066	0.4060±0.0066	0.4785±0.0094
c4	0.1644±0.0076	0.9208±0.0076	1.0853±0.0108
Average	0.0729±0.0057	0.4081±0.0057	0.481±0.0114

Table B4: Results of external and internal Hazard indices, and radioactivity level index.

Code	H_{ex}	H_{in}	I_{γ}
a1	0.4768±0.0335	0.5667±0.0502	1.2283±0.0048
a2	0.5467±0.0453	1.0030±0.0900	1.3759±0.0125
a3	0.0787±0.0052	0.0910±0.0073	0.2163±0.0002
a4	0.1295±0.0099	0.1527±0.0153	0.3468±0.0007
a5	0.2957±0.0260	0.4629±0.0492	0.7517±0.0042
a6	0.5202±0.0711	0.7352±0.1414	1.3292±0.0308
a7	0.4342±0.0558	0.5846±0.0563	1.1140±0.0209
a8	0.1341±0.0230	0.2076±0.0455	0.3508±0.0033
a9	0.0667±0.0039	0.1083±0.0071	0.1779±0.0001
a10	0.0720±0.0083	0.1141±0.0158	0.1905±0.0004
b1	0.1997±0.0178	0.3255±0.0309	0.5064±0.0020
b2	0.6496±0.1259	0.7776±0.1520	1.6794±0.0933
b3	0.2909±0.0434	0.4675±0.0776	0.7449±0.0065
b4	0.2579±0.0562	0.3637±0.1011	0.6620±0.0197
c1	0.4713±0.0390	0.7356±0.0735	1.1962±0.0094
c2	0.6110±0.0659	0.8427±0.1035	1.5670±0.0278
c3	0.3598±0.0530	0.5934±0.0992	0.9124±0.0174
c4	0.7976±0.0487	1.0333±0.0782	2.0438±0.0151
Average	0.3551±0.0407	0.5092±0.0663	0.9108±0.0150

Table B5: Results of concentration activities for ^{235}U through its daughter nuclide ^{227}Th .

Code	Nuclide	Peak	Activity concentration($BqKg^{-1}$)
a1	Th-227	256.25	0.376±0.110
a5	Th-227	286.15	3.550±0.759
a6	Th-227	299.9	3.503±0.229
a6	Th-227	304.35	5.819±0.381
b3	Th-227	329.82	2.509±0.150
Average			3.151±0.326

Appendix C

Table C1: Results of concentration activities for J_{135} .

Code	$A_{J_{135}} (BqKg^{-1})$
a2	44.604±10.527
a3	49.207±4.196
a4	142.468±12.708
a5	40.855±13.021
a7	10.928±1.189
b1	1.540±0.23
b2	66.067±9.452
b3	101.523±16.655
c1	158.575±9.53
c2	50.194±7.73
Average	66.596±8.524

Table C2: Effluents activity concentrations of nuclear events in samples.

Contamination nuclides	Average over samples ($BqKg^{-1}$)
Nb-95	1.242±0.135
Mo-99	116.001±15.161
Sb-125	42.351±12.934
J-131	14.01±0.7
Cs-134	134.756±32.867
Ba-140	34.977±8.181

References

1. Wagenaar, D.J. 2.2.3 *Radioactivity in Equilibrium* 1995 October 6; Available from: www.med.harvard.edu/JPNM/physics/nmltd/radprin/sect2/2.2/2_2.3.html.
2. Parks, J.E. *The Compton Effect--Compton Scattering and Gamma Ray Spectroscopy*. 2015 6/01; Available from: <http://www.phys.utk.edu/labs/modphys/Compton%20Scattering%20Experiment.pdf>.
3. Kirz, J., *X-Ray Data Booklet; Section 3.1 SCATTERING of X-RAYS from ELECTRONS and ATOMS*. p. section 3-1.
4. ORTEC®, *905 Series NaI(Tl) Scintillation Detectors*.
5. ORTEC. *MCA. The Multichannel Analyzer*. . 2010-2014; Available from: ©Copyright 2010-2014 AMETEK, Inc. All Rights Reserved. www.ametek.com.
6. NDT. *NDT RESOURCE CENTER. Energy, Activity, Intensity and Exposure* Available from: <https://www.nde-ed.org/.../RadiationSafety/theory/activity.php>.
7. University, I.S. *Radiation Related Terms* Available from: www.physics.isu.edu/radinf/terms.htm.
8. CDC. *Emergency Preparedness and response*. Available from: emergency.cdc.gov/radiation/glossary.asp.
9. Flakus, F.N., *Detecting and measuring ionizing radiation - a short history*. IAEA BULLETIN. **23**(4).
10. ICRP. *ICRP International Commission on Radiological Protection* Available from: www.icrp.org.
11. ACS, A.c.s. *Evolution of cancer treatments: Radiation*. 2014 06/12/2014; Available from: <http://www.cancer.org/cancer/cancerbasics/thehistoryofcancer/the-history-of-cancer-cancer-treatment-radiation>.
12. IAEA. *International Atomic Energy Agency (IAEA)*. Available from: <https://www.iaea.org>.
13. UNSCEAR, *ANNEX B Exposures from natural radiation sources*. 2000. p. 115-116.
14. Stratamodel. *Uranium Exploration - Gamma Soil Survey: Full Soil Survey Services*. 2016; Available from: <http://www.stratamodel.com/gamma.htm>.
15. Commons, W. *Decay chain(4n+2, Uranium series).svg*. 2015 11 June; Available from: <https://commons.wikimedia.org/w/index.php?curid=33293646>.
16. Commons, W. *Decay Chain Thorium.svg*. 2015 3 December]; Available from: <https://commons.wikimedia.org/w/index.php?curid=16983885>.
17. Wikipedia. *Decay chain*. 2008; Available from: <https://www.wikipedia.org/search-redirect.php?search=actinium>.
18. Reitz, J.R., F.J. Milford, and R.W. Christy, *Foundation of Electromagnetic Theory*. 1993: p. 525-535.
19. Jackson, J.D., *Classical Electrodynamics*. 1999: p. 407-449.
20. Dokhane, D.A. *PHYS 580, KSU, 2007 1 PHYS 580 Nuclear Structure Chapter 5-Lecture1 Gamma Decay*. 2007; Available from: slideplayer.com/slide/5806216.
21. Cohen, B.L., *Concepts of nuclear physics*. 1971, New Delhi: TATA McGRRAW-HILL PUBLISHING COMPANY LTD. 30.
22. Ragheb, M. *Gamma Rays Interaction with matter*. 30/10/2013; Available from: <http://mragheb.com/NPRE%20402%20ME%20405%20Nuclear%20Power%20Engineering/Gamma%20Rays%20Interactions%20with%20Matter.pdf>.
23. Serman, N. *Production of X-rays and Interactions of X-rays with Matter*. Available from: http://www.columbia.edu/itc/hs/dental/sophs/material/production_xrays.pdf.
24. Knoll, G.F., *Radiation Detection and Measurement*. 2010: John Wiley & Sons. 306-328.
25. Cure, N. *3 Big Reasons to Choose Natural Cures and Natural Remedies Over Orthodox Medical Treatments*. Available from: <http://www.life-saving-naturalcures-and-naturalremedies.com/#sthash.AebVwzLg.dpuf>.

26. Barth, R.F., et al., *Current status of boron neutron capture therapy of high grade gliomas and recurrent head and neck cancer*. Radiation Oncology, 2012. **7**(1).
27. National Cancer Institute. *Radiation Therapy for Cancer* Available from: [www.cancer.gov/about-cancer/treatment/types/radiation-therapy/...](http://www.cancer.gov/about-cancer/treatment/types/radiation-therapy/)
28. Hasan, F., *Natural Alpha Particle Radioactivity In Soil In Hebron*. Hebron University Research Journal, 1999. **1**(1).
29. Dabayneh, K.M., *Assessment of Natural and Man –Made Radioactivity Levels of the Plant Leaves Samples as Bio- Indicators of Pollution in Hebron District- Palestine*. Arab J. of Nuclear Science and Applications, 2006. **39**(2): p. 232-242.
30. Thabayneh, K.M. and M.M. Jazzar, *Radioactivity Levels in Some Plant Samples in the North Western of West - Bank , Palestine and Evaluation of the Radiation Hazard*. Rad. Prot. Dos., 2013. **153**(4): p. 467–474.
31. Dabayneh, K.M., *Radioactivity Measurements in Different Types of Fabricated Building Materials used in Palestine*. Arab J. of Nuclear Science and Applications, 2007. **40**(3): p. 207-219.
32. Dabayneh, K.M., A. Sroor, and S. Abdel-Haleem, *Environmental Nuclear Studies of Natural and Manmade Radioactivity at Hebron Region in Palestine*. Al-Quds Univ. J. for Research and Studies, 2008. **12**: p. 23-42.
33. Dabayneh, K.M., *Natural Radioactivity in Different Commercial Ceramic Samples Used in Palestinian Buildings as Construction Materials*. Hebron University Research J. (A) (Natural Science), 2008. **3**(2): p. 49-58.
34. Dabayneh, K.M., L.A. Mashal, and F.I. Hasan, *Radioactivity concentration in soil samples in the southern part of the West Bank, Palestine*. Radiat Ion Protection Dosimetry, 2008. **131**(2): p. 265–271.
35. Thabayneh, K.M. and M.M. Jazzar, *Natural Radioactivity Levels and Estimation of Radiation Exposure in Environmental Soil Samples from Tulkarem Province-Palestine*. Open Journal of Soil Science, 2012: p. 8-16.
36. Thabayneh, K.M., et al., *Determination of Natural Radioactivity Concentrations and Dose Assessment in Natural Water Resources from Hebron Province, Palestine*. Hebron University Research J. (A), 2012. **6**: p. 19 – 33.
37. Thabayneh, K.M., *Measurement of Natural Radioactivity and Radon Exhalation rate in Granite samples Used in Palestinian Buildings*. Arab J Sci. Eng., 2013. **38**(1): p. 201–207.
38. Jazzar, M.M. and K.M. Thabayneh, *Transfer of natural radionuclides from soil to plants and grass in the western north of West Bank environment- Palestine*. International Journal of Environmental Monitoring and Analysis, 2014. **2**.
39. ABU SAMREH, M.M., K.M. THABAYNEH, and F.W. KHRAIS, *Measurement of activity concentration levels of radionuclides in soil samples collected from Bethlehem Province, West Bank, Palestine* Turkish Journal of Engineering & Environmental Sciences, 2014 p. 113-122
40. Thabayneh, K.M., *Soil-to-Plant Transfer Factors and Distribution Coefficient of Cs-137 in Some Palestinian Agricultural Areas*. Open Access Library Journal, 2015.
41. Thabayneh, K.M., *Determination of Alpha Particles Concentration in Some Soil Samples and the Extent of their Impact on the Health*. Sains Malaysiana Journal, 2016. **45**(5): p. 699-707.
42. Thabayneh, K.M., et al., *Radionuclides Measurements in Some Rock Samples Collected from the Environs of Hebron Region–Palestine*. Jordan Journal of Physics, 2016. **9**(1).
43. Finder, W.M., *west bank*. 2015.
44. ALDRICH, S. *Thallium Iodide CRYSTAL GROWTH GRADE*. Available from: www.sigmaaldrich.com/content/dam/sigma-aldrich/...

45. NUCSAFE. *Selecting Gamma Detector*. 2016; Available from: <http://www.nucsafe.com/cms/Selecting+Gamma+Detector/43.html>.
46. Derenzo, S., et al. *Scintillation Properties*. 2015 October 23; Available from: <http://scintillator.lbl.gov/?con&dom=pscau&src=syndicationor%20scintillator.lbl.gov>.
47. Hossain, I., N. Sharip, and K. Viswanathan, *Efficiency and resolution of HPGe and NaI(Tl) detectors using gamma-ray spectroscopy*. Scientific Research and Essays, 2012. **7**(1): p. 86-89.
48. ORTEC, *Gamma-Ray Spectroscopy Using NaI(Tl)*.
49. El-Khatib, A.M., et al., *Calculation of full-energy peak efficiency of NaI (TI) detectors by new analytical approach for parallelepiped sources* Journal of Theoretical and Applied Physics, 2013. **7**(2): p. 11.
50. Erees, F.S., et al., *Assessment of dose rates around Manisa (Turkey)* Radiation Measurements, 2006. **41** (5): p. 598-601.
51. Huy, N.Q. and T.V. Luyen, *Study on external exposure doses from terrestrial radioactivity in Southern Vietnam*. Radiat Prot Dosimetry, 2006. **118**(3): p. 331-6.
52. Rafique, M., *Cesium-137 activity concentrations in soil and brick samples of Mirpur, Azad Kashmir; Pakistan*. International Journal of Radiation Research, 2014. **12**(1).
53. Sandatlas, *Composition of the crust*.
54. Harb, S., et al. *CONCENTRATION OF U-238, U-235, RA-226, TH-232 AND K-40 FOR SOME GRANITE SAMPLES IN EASTERN DESERT OF EGYPT*. in *Proceedings of the 3rd Environmental Physics Conference*. 2008. Aswan, Egypt.
55. Malek, M.A., K.J.A. Chisty, and M.M. Rahman, *Radiological Concentration Distribution of I-131, I-132, I-133, I-134, and I-135 Due to a Hypothetical Accident of TRIGA Mark-II Research Reactor*. Journal of Modern Physics, 2012. **03**(10): p. 1572-1585.
56. Trinh Van, G., et al. *Observation of Radionuclides from Fukushima Nuclear Accident T1-P42 at Some Environmental Radiation Monitoring Stations in Vietnam*. in *Science and technology 2013 conference*. 2013. Hofburg Palace, Vienna, Australia.

قياسات أشعة جاما لعينات من التربة في الأجزاء الجنوبية لبنت لحم وحتى الأجزاء الجنوبية من الخليل في فلسطين

ملخص:

هَدَفْنَا في هذه الدراسة الى التعرف على قيم النشاط الاشعاعي بالنسبة للمكان، حيث قمنا بجمع 4 عينات من الشريط الجنوبي لمحافظة بيت لحم و 4 عينات من الشريط الشمالي لمحافظة الخليل و 10 عينات من الشريط الجنوبي و في كل شريط أخذت العينات من الشرق الى الغرب. تم قياس هذه العينات باستخدام مجس الوميض الاشعاعي "يوديد الصوديوم المُطعم بالثاليوم". و بعد اجراء التعديلات الحسابية، حصلنا على قيم النشاط الاشعاعي لكل من السلاسل الرئيسية المشعة طبيعياً المتمثلة في سلسلة اليورانيم-238 و 235 و سلسلة الثوريوم-232 و نظير البوتاسيوم-40 الطبيعي الاشعاع، و نظير السيزيوم المنتج صناعياً و معدلات النتائج المتحصلة عبر العينات لهذه النظائر كانت على التوالي هي (57.0±9.7) و (3.151±0.326) و (47.9±6.0) و (78.0±8.9) و (1.2±0.1)، بيكويرل/كغم و هذه القيم تقع ضمن مديات القياسات العالمية و مقاربة لمعدلاتها و موافقة لها.

اضافة الى ذلك تم حساب القيم المعيارية المرتبطة بالنشاط الاشعاعي والتي تبين مدى خطورة التعرض لهذا و لغيره من المستويات، و هذه القيم باختصار هي النشاط الاشعاعي المكافئ للراديوم بدلالة نشاط اليورانيم 238 و الثوريوم 232 و البوتاسيوم 40، و قيمتها المتحصلة هي (131.5±15.1) بيكويرل/كغم، و الجرعة الشعاعية الممتصة هوائياً على ارتفاع متر واحد فوق سطح الارض المأخوذة منها العينة و ذلك بدلالة النظائر الثلاث المذكورة سابقاً و قيمتها المتحصلة هي (59.4±6.7) نانو جراي/الساعة، كما تم حساب نفس القيمة اذا ما اعتبرنا أثر السيزيوم 137 و قيمتها المتحصلة هي (93.4±6.7) نانو جراي/الساعة، القيمة التالية كانت الجرعة الفاعلة حيويًا و المُقدرة حويلاً و المعتمدة على الجرعة الممتصة هوائياً بعلاقة خطية و قيمتها المتحصلة هي (0.481±0.01140) ميلي سفارت/سنة، و هذه القيم التابعة خطياً لنشاط النظائر الطبيعية السابقة الذكر هي تابعة لها ايضاً في توافقها مع القيم العالمية. القيمة التالية هي مؤشر المخاطرة للتواجد في الاماكن المفتوحة بدلالة النشاط الاشعاعي المكافئ للراديوم و قيمتها المتحصلة هي (0.3551±0.0407) و يليها مؤشر المخاطرة للتواجد في الاماكن المغلقة بدلالة النشاط الاشعاعي المكافئ للراديوم و قيمتها المتحصلة هي (0.5092 ± 0.0663)، و القيمة الاخيرة هي مؤشر مستوى النشاط الاشعاعي بدلالة الجرعة الفاعلة حيويًا و المُقدرة حويلاً و قيمتها المتحصلة هي (0.9108±0.0150)، هذه القيم الثلاث الاخيرة هي نسبية، قيمتها العليا واحد صحيح و وصولها و تجاوزها لهذا الحد يعني ان قياساتنا و الحسابات المبينة عليها تشير الى ان المنطقة المدروسة تُعرض المتواجد فيها للاصابة بالامراض الناتجة عن الاشعاع، اي ان القيم المحصلة المبيّنة اعلاه جائت ضمن معايير السلامة و مقاربة للقيم الدولية.

اضافة الى ذلك تم التعرف على الكثير من نظائر الدفق النووي الناتجة عن نشاطات مفاعلات انتاج الطاقة النووية والتجارب النووية القائمة حول العالم في فضاء الارض و حديثاً منذ الستينات تقريباً في جوفها و تحت البحر بشكل دقيق مجوقل و دفق سائل و الذي يؤدي الى التلوث بالوصول الى الاماكن المأهولة و بالتسرب الى المياه الجوفية و الى مياه البحار التي ترسله الى الانسان بطرق عدة، و هذه المواد المتسربة ترتبط بانواع التفاعلات المُحَبَّدة في انتاج الطاقة و الاسلحة النووية و من النواتج التي وجدناها في العينات بشكل واسع هو نظير J-135 بمعدل نشاط اشعاعي عبر جمع العينات مقداره (66.596±8.524) بيكويرل/الثانية و النظائر (NB-95, MO-99, SB-125, J-131, Cs-134, BA-140) بمعدل نشاط اشعاعي لكل منها كما يلي بالترتيب تتابعاً (116.001±15.161, 1.242±0.135, 34.977 ± 8.181, 134.756± 32.867, 14.01± 0.7, 42.351±12.934).